IMPLEMENTATION AND HARMONIC ANALYSIS OF DQ-CONTROL ON A GRID-TIED SINGLE PHASE INVERTER FOR PHOTOVOLTAIC SYSTEMS IN A DISTRIBUTION NETWORK

by

Robin Pratap Singh Bisht

A thesis submitted to the faculty of
The University of North Carolina at Charlotte
in partial fulfillment of the requirements
for the degree of Master of Science in
Electrical Engineering

Charlotte

2016

Approved by:

_____
Dr. Sukumar Kamalasadan

_____
Dr. Abasifreke Ebong

_____
Dr. Maciej Noras

ABSTRACT

ROBIN PRATAP SINGH BISHT. Implementation and harmonic analysis of dq-control on a grid-tied single phase inverter for photovoltaic systems in a distribution network. (Under the direction of DR. SUKUMAR KAMALASADAN)

The electrical utilities are very much concerned about the power quality due to the presence of nonlinear loads in their power distribution systems. The non-linear residential loads cause harmonics in the residential distribution systems. To mitigate the harmonics, active or passive filters are normally used. Past decade has seen a rise in the installation of DGs in residential areas. Especially renewable energy based DG's such as Photovoltaic (PV). In this thesis we focus on an existing model of a distribution network present in Netherlands (Vernormeer 4), and discuss the impact of harmonics on the system and how we can mitigate these harmonics by using active filtering methods. The passive filters utilize the passive components such as Inductors, resistors and capacitors and the active power filters utilize the power electronic switches for the harmonic compensation. The active filters are advantageous than the passive filters because it can eliminate focused or a wide range of harmonics in the system where as passive filters compensate specific order harmonics. The example for the active filter is the inverter, in which the controlled switching of the inverter compensates the harmonics in the specified system. Traditional methods of control on the inverter are still a cushion most of the manufacturers fall back on, but these types of inverters have major issues. They utilize the voltage supply for the reference wave generation and synchronization which in itself might be polluted and hence polluting the injected current into the grid. We implement a dq-control methodology on the inverter, which has been a focal point for researchers nowadays on inverter control. In this

thesis, we jump into the dq-control architecture and see how it performs on the grid-connected mode and investigate the harmonic problems that are existent in almost every distribution network. We also try providing a framework for future research on mitigation and further analysis on several power quality problems.

ACKNOWLEDGEMENTS

Working on this area of research has been a great experience and for that I would like to thank the people involved in the formulation of this thesis. Firstly, I want to thank my parents who have been a constant support and have laid the foundation to the person I have become. They have been with me through everything, good and bad.

I would like to express my utmost gratitude to my advisor, Dr. Sukumar Kamalasadan for his guidance and support during these two years of my master's studies. His patience and constant encouragement have really helped me to go through this process and learn to think through the toughest problems.

I sincerely thank the committee members Dr. Abasifreke Ebong and Dr. Maceij Noras for taking time to be on my committee and assess my work.

I would like to express my gratitude to Dr. Yamilka Baez-Rivera. She has been there as a friend and has helped me out a lot on my research work. I am thankful to my friends for their love and support. They have been there throughout, during my best and my worst.

Finally, I would like to thank all the professors and staff at the University of North Carolina at Charlotte who have contributed in enriching my knowledge.

TABLE OF CONTENTS

CHAPTER 1 : INTRODUCTION

The penetration of single phase grid connected PV systems has been ever rising since the past couple of decades, commercially and in residential areas. The rise in the density of PV systems in a particular area pose numerous problems; notably, power quality and reliability. Grid interconnection requirements and specifications have been strengthened to overcome these issues, but more research and deep insight into the problems have to be done in order to establish robust ground rules. Coming times will see more active involvement of single phase grid connected PV systems and the control designs should be able to provide both power quality and reliability as stated in IEEE 1547. For example, the total harmonic distortion (THD) for the grid current should be below 5%.

Due to the specifications imposed by the IEEE the control methodologies aim to provide Low voltage ride through (LVRT) and maintain the grid interconnection regulations. In order to reduced or eliminated current and voltage distortion, simple PI-based αβ controllers have been implemented before. But achieving zero steady state error is difficult; Although, PI-based dq control have been used on 3 phase systems to eliminated the zero steady state error problem and also achieve control on the power factor. However, in single phase grid connected system, these controllers cannot be applied directly because of the missing quadrature element.

Distributed power inverters have many sections doing various things which contribute to either the synchronizing with the grid, dc–ac power conversion; reactive power compensation; harmonic cancellation; protection against islanding; UPS operation; etc. In some cases, these controllers are implemented in multitasking converters. The control references are usually internally generated and are synchronized with the grid voltage, this synchronization is done via PLL. But some of the inverters combine the reference source and the synchronization with the supply voltage by using the waveform shape of the supply voltage as a reference source. If the voltage source used as a reference is polluted with background distortion, the reference will also be distorted hence the internal control loop using current reference will inherit this distortion. Distortions can also be mitigated by the use of active and passive filters. Filter design is technique often used for improving loadability, improving voltage regulation, power factor correction etc. Filter banks are used in transmission as well as distribution lines. Although they cannot be used everywhere and the flexibility they provide is minimal. Active power filtering methods are taken over and are discussed in [34]. Both in single and three phase systems, active power filters have enormous contributions to voltage quality problems, unbalanced currents, poor power factor etc. Distribution static compensators (DSTATCOMs) are used for eliminating these problems and is now a mature technology.

In this thesis, we are contributing to provide a framework for understanding harmonic peaking in a distribution system with the rise of PV penetration and also enter the areas of understanding mitigation techniques of these harmonics using active power filters. This framework will provide a path for future research in mitigation and

investigation for power quality problems associated with distributed energy generation with photovoltaics.

1.1. Control Architectures on Single Phase Inverter System

Extensive work has been done already on this domain aimed to control the output voltage with good dynamic response and zero steady state error. Many control methodologies have been formed and utilized over the years. Some of them are:

- Hysteresis control method utilizes the inverter output current and is controlled in a hysteresis loop. The current follows a current reference, which is limited by the bands of the hysteresis loop. The switching of the inverter's legs is based on the current touching the limits of the band, which limits the peak current. This type of control is ineffective because the PWM switching is varying because the current peak-peak ripple is to be controlled all the time and therefore we often notice a high THD where this controller is used. Although, the efficiency of this control can be increased by optimizing the hysteresis band with respect to its load parameters, but there is a trade off with a high variation of PWM switching frequency.

- Synchronous reference frame controller, is an important controller scheme for our research as the current error compensation design has been proposed for this study. Regulated vectors are rotated into the synchronous reference frame to that of the fundamental output frequency. We can say that the DQ control methodology is the next step to this architecture.

- DQ reference frame controller, in three phase systems this controller is utilized for zero steady state errors. Converting the inverter current output to their respective d components and q components and evaluating the error signal from the references (either dc-link voltage or reactive power or dq components of the grid side voltage) we use PI controllers to generate the reference signal for the pulse width modulation. In literature, these methods have been successfully implemented on grid tied inverters.

1.2. Power Quality

Power quality generally means to maintain good quality of power at the generation level, transmission, distribution and consumer level throughout. Power supply systems since have been polluted and is much sever at the consumer level. It is important to study these problems and the terminals. Often pollution of the supply systems is caused by natural reasons, which contribute to 60%, and the rest are forced ones.

Non-linear loads and elements produce harmonics and consume reactive power. If there is no proper compensation, they can deteriorate power quality of ac systems. Usually, power quality problems are related to the voltage at the PCC where these loads are connected. The power quality problem has become more severe due to the introduction of solid state devices. These devices come at a price, although they have made technology reduce in size and cost and more efficient, but pollution in the grid is an innate quality and these devices are highly susceptible to these distortions and they produce it themselves. For grid-connected inverter the current distortion is a huge threat and it is stated in IEEE

1547 that the THD of the grid current should be <5%, for 3rd to 9th harmonics the limit is 4% and the even harmonics are limited to 25% of the odd harmonic limits.

The presence of low-order harmonics on the grid side voltage and inverter output voltage results in the injected current being distorted. Control methodologies implemented should take care that the controllable output voltage of the inverter that theoretically can cancel out the harmonic content present in the grid. On assumption that the grid is clean, we can say that the only contribution to the power quality or harmonic generation problem is the inverter. Inverter output voltage consists of the fundamental component and harmonics which are induced by the PWM. The injected current into the grid will inherit these harmonics. The inverter output voltage will distort the grid voltage partially by the inverter PWM and the dc-link voltage fluctuations. Other sources include the anti-islanding algorithms used in PV grid-tied inverter systems which use the grid voltage as reference, not only here but also in reference wave generation for PWM, which is inevitably corrupt the injected current into the grid.

There is a need to limit or control the distortion at the consumer level, because the customer's devices and equipment have become more susceptible to these power quality problems than ever before due to the use of power electronic converters. In the wake of these problems a wide range of mitigation techniques have arisen, such as passive filters which include passive components and can be classified in to series and shunt filters, and active filters which use power electronic converters itself generating the reference harmonics to mitigate them.

Passive filters are often used in ac networks to absorb harmonic currents, and are extensively used because they are cheap and efficient. They have their drawbacks, they are susceptible to resonance and they are heavy and often become inefficient when they are used for long periods of time.

1.3. Passive Filters

There are two types of passive filtering methods, series and shunt, which is now a mature technology. It provides transient, steady state, dynamic, voltage and angle stabilities. These filters can work either individually or in combination, the type can be determined by the requirement of the system. Their classification is based on:

- Topology, like mentioned before, passive filters can work in series, shunt or hybrid.
- Supply system based, this classification of passive filters is based on the supply or the load systems, which are either single phase or three phase systems. Loads can be single phase, or three phase with or without neutral connection. Passive compensators provide load balancing and reactive power compensation so it is important to understand the system that we are dealing with.

Shunt compensators provide reactive power compensations and improve the voltage profile at the PCC or wherever they are placed in the network. They are often used in stand-alone distributed power generating systems.

Series compensators are used for voltage regulation and power flow control. Although they have problems dealing with resonance and also if they are connected in series with loads, they affect the voltage across the loads. Hence caution must be taken using series compensation. Mostly they are used in combination with the shunt filters.

1.4. Active Filters

Primitive technology such as the VAR compensators have been used to eliminated various power quality problems, but active filters are emerging in recognition not only due to their efficiency but also due to their wide range of application. Active power filters (APF) provide reactive power compensation, load balancing and harmonic compensation. APFs are classified on the topology, type of system and the converter which is used.

- Converter based, APFs uses two types of converters, current source converter (CSC) and voltage source converter (VSC).

- Topology based, APFs with half-bridge topology, full-bridge topology and H-bridge topology.

- Supply system based, the supply or the load system has a role to play in what type of active filters is to be used.

The control of APFs is usually based on the estimation of the reference currents using feedback signals. The reference current signals and the sensed signals are then used in control strategies to develop the PWM gating signals for the VSC used as a APF. The control algorithms used for the control of these VSCs are categorized into time-domain and frequency domain. Some of them are as follows:

- Single phase DQ theory

- Single phase PQ theory

- Neural network theory

- PI controller-based theory

- Adaptive detecting control algorithm

- Fourier series theory

- Recursive discreter Fourier transform theory

- Kalman filter-based control algorithm

This thesis is organized as follows:

- Chapter 2 describes various inverter topologies and the elements used in it. Grid-tied inverters have to follow several rules for interconnection with the grid, which is explored in this chapter.

- Chapter 3 presents the theoretical aspects of the single phase inverter system in the dq-reference frame. The dq-controller architecture for a single phase inverter is developed in this chapter which is derived from the orthogonal signal generation theory.

- Chapter 4 describes the VP4 system which is considered for our research and on which our PV inverter system is implemented. Hardware capabilities of RTDS have been explored and IEEE1547 tests were performed on the inverter.

- Chapter 5 presents the on- and off-grid simulation results of our PV inverter system in the VP4 network. We assess the harmonic content and compare the results with [6]

- Chapter 6 presents conclusion and future work.

CHAPTER 2 : INVERTER TOPOLOGY AND INTEGRATION

This chapter explains the topology of inverter used and the types of PWM considered and equipped for the simulation purposes. Designing the system in RSCAD is quite different from the other simulation software, so the process of creating the signals is explained in this chapter. Also, this chapter includes the integration standards and regulations for distributed generators.

2.1. Inverter Topology

Photovoltaics are important contributors to power generation nowadays and due to their DC nature we need DC to AC power conversion. The aim of creating a reliable AC voltage source is done by the inverter and are often used when the generation in AC and as uninterruptible power supply everywhere. Here, for the UPS operation, reliability and the quality of the power matters hence there is a need to have a good robust control architecture to prevent disruptions.

Distributed power are based on single phase voltage source inverter and in certain cases high-frequency transformers are used. In this study we have used a transformerless topology, a simple H-bridge inverter. In RTDS, the small time step elements have to be modelled separately, hence we use an interfacing transformer to connect it to the large time step devices as shown in Fig. 2.1.

Single phase full-bridge inverter of Fig. 2.1 is used to convert DC to AC using a particular sequence of swtiching of the gates. Output voltage of the inverter is +Vdc,-Vdc or 0 depending upon the control on the switching. Both the switches on one leg operate at different times, this is due to the fact that if both of the switches are operated at the same time it will create a short circuit condition.

The switching devices consists of a semiconductor switch and an anti-parallel diode. As and when the switching frequency is increased, we get a wave on the inverter output closer to a sine wave, but the trade off is switching losses and this is an important part of the design process, and bi-directional switches especially need to have lower losses. MOSFETs and IGBTs are usually used in inverters due to their robustness in high power applications.

The inverter operates on either uni- or bipolar with PWM; unipolar is better than bipolar switching due to the fact that the ripple content is lesser. In bipolar switching the upper and lower swtiches in the same leg operate complementary to each other and all switches operate at the same time, whereas in unipolar the upper two switches do not work simultaneously.

For our research, we have used bipolar modulation with a basic H-bridge inverter in order to test the functioning with the grid being clean and with harmonic content.

2.2. PWM Switching

The technique here used is Bipolar PWM switching. This is achieved by creating the reference wave and compared to the triangular wave, as shown in figure 2.2. The upper and lower switches of one leg are switched complementary to each other. All the switches

are turned on and off at the same time. The output of one leg is equal and opposite to the output of the other leg. In RTDS, the signals that are sent to the switches are done by the firing pulse generator with the combination of a triangular wave generator as shown in figure 2.3.

The values TANGLE1 and TOMEGA1 come from mathematics, TOMEGA1 controls the frequency of the carrier wave and TANGLE1 handles the phase of the triangular wave. Usually the angle is synched with the grid and the omega is 2*pi*60. The generation of these values are shown in figure 2.4. There can be N valves in RTDS and N valves are controlled by N consecutive bits in a firing pulse word.
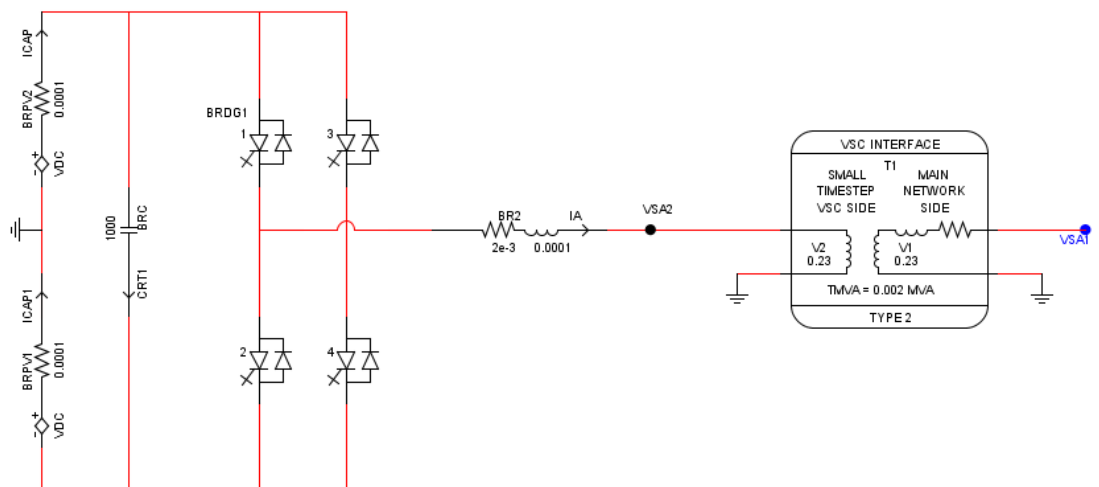
FIGURE 2.1 Single phase inverter with the interfacing transformer
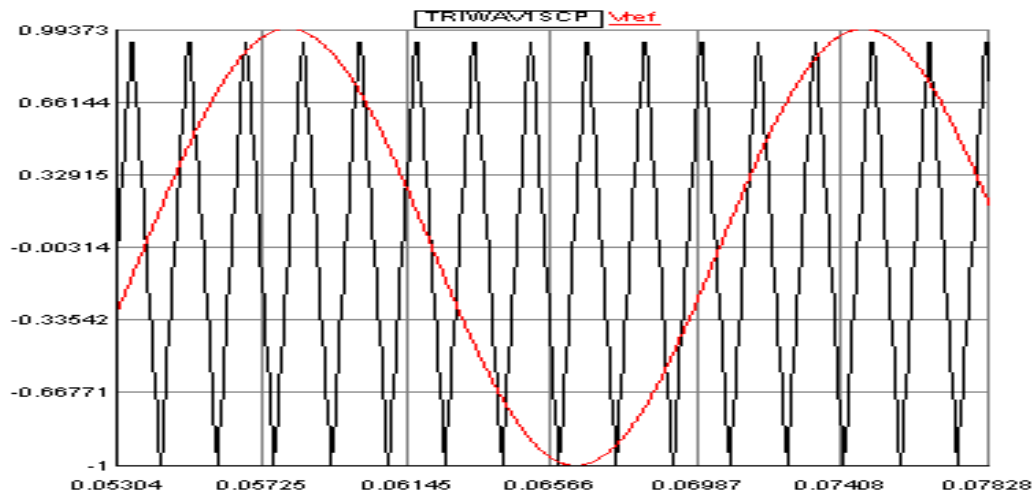
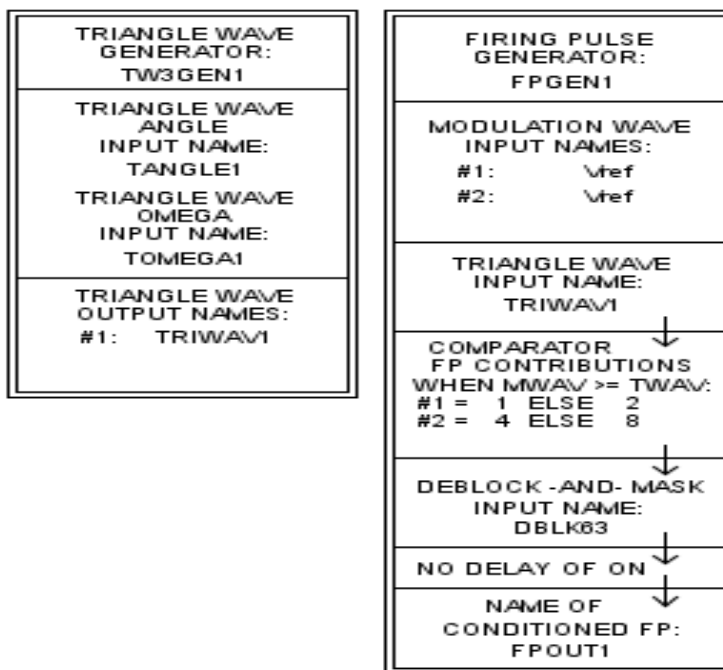Figure 2.2. Reference wave and the triangular wave

FIGURE 2.3: Firing pulse generation and triangular wave generation in RTDS

The figure 2.3, shows how we have generated the waveforms required for our PWM, and the FPOUT1 signal is essentially the pulses given as the firing pulse word, as discussed before, to the MOSFETS.
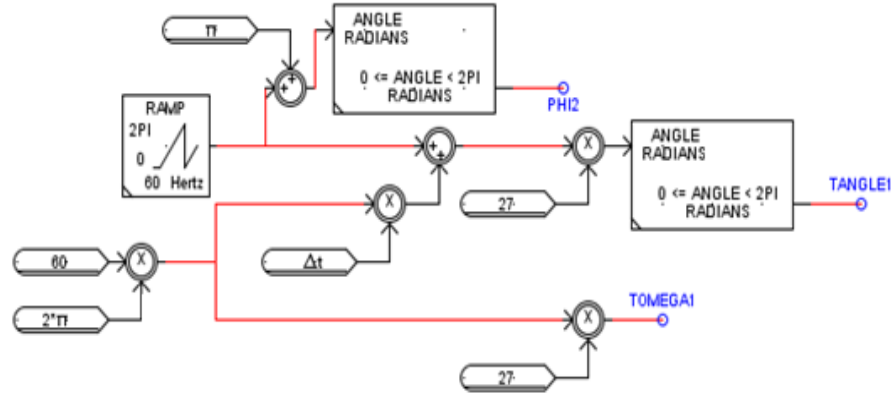
FIGURE 2.4 Generation of the triangular wave parameters

2.3. Inverter Output Filters

Manufacturers try to be cost effective and usually wind up reducing the reactor size and increasing the output capacitor. The output capacitor is responsible to set up a resonance circuit with the network elements and cause certain harmonics to peak. This is often overlooked by the manufacturers and we have decided to stick with that in order to analyze the harmonic content in the system. In commercial power inverters (1-3 kW) the typical values of the output capacitance used is 0.5-10uF. Hence, in this study passive filters were not designed but are abided by the range as mentioned above. LC-filter is used, since it is less complicated and abides by the range we have assumed, we see the performance of the LC filter by looking at the bode plot in figure 2.5.

The switching frequency used for the simulation is 20kHz and the cut off frequency usually for the passive filter should be 1/6th of the switching frequency. As we do not have the luxury to assign the values, we see that the cut off frequency is a bit higher. The calculated cut off frequency is 3kHz and the cut off frequency from the bode plot is 6kHz.
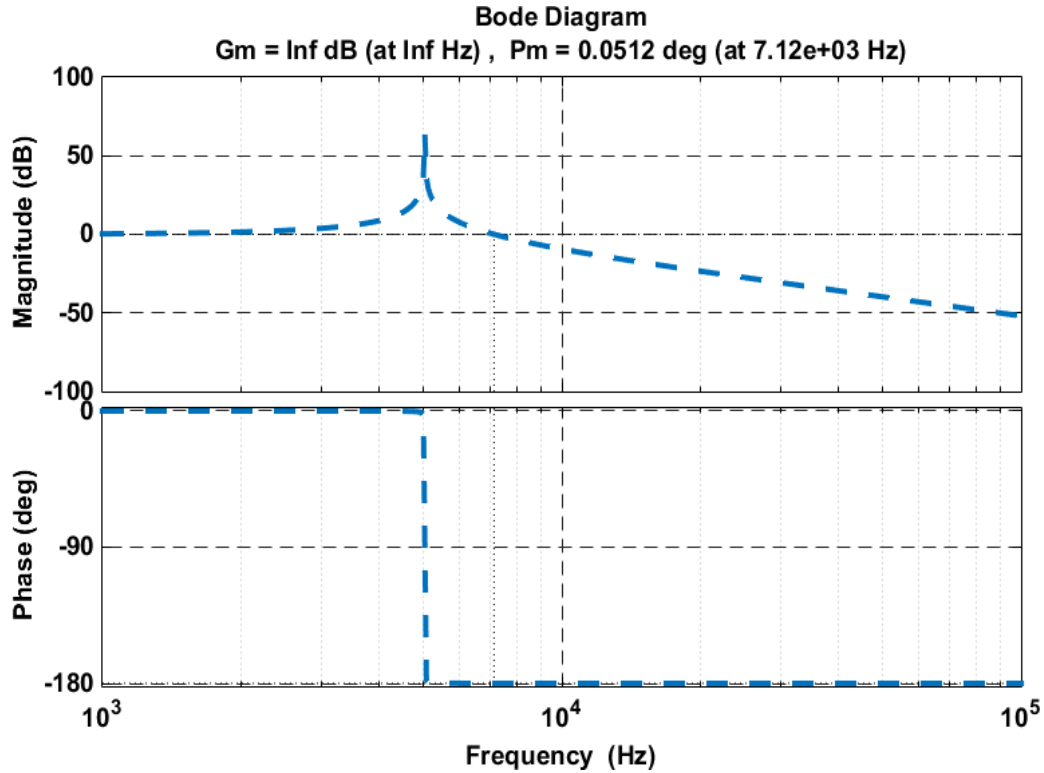
Bode Diagram

Gm = Inf dB (at Inf Hz) , Pm = 0.0512 deg (at 7.12e+03 Hz)

FIGURE 2.5: LC filter bode plot

TABLE 2.1 Filter values and frequencies

L	C	Fswitching	Fcutoff
0.1 mH	6 uF	20kHz	6kHz

2.4. Grid Connection Standards

Designer responsible for the interconnection of grid-tied inverter should be aware of the standards and regulations for the interconnection. There is an international committee that decides and implements these rules, namely the Institute of Electrical and Electronics Engineers (IEEE). The standards for the grid interconnection are mentioned in IEEE Std. 1547. Where, this standard gives guideline and explains the limitation for the interconnection of the distributed generation.

There are many requirements stated in the IEEE 1547, we here have a look on the interconnection guidelines,

- Anti-islanding, the definition according to the IEEE for anti-islanding is:

  An inverter will cease to energize the utility line within 10 cycles or less when subjected to a typical islanded load.

  Although, this does not encapsulate the whole idea for anti-islanding feature, but the provides us with the knowledge that islanding needs to be dealt pragmatically. The inverter should cease to energize the utility line under 2s when the quality factor of the line is 2.5 or less.

- Voltage, response to abnormal voltage on the PCC is more of a protection scheme for the inverter. The voltage detection and the trip times are shown in table 2.2.

TABLE 2.2 Voltage operating range and trip times (trip timings are after the detection of the abnormality in the voltage in order to keep a buffer for future reconnect)

Voltage	Trip Time
V<50%	0.16
50%<V<88%	2
110%<V<120%	1
120%<V	0.16

- Frequency, if there are any abnormalities on the grid side in regards to frequency, the PV inverter system shall cease to energize the grid. The standard for clearing times for the frequency abnormalities are mentioned

in table 2.3. If the gird stabilizes before the clearing times, the PV inverter system does not cease and continues its operation.

TABLE 2.3 Frequency range and clearing time (the clearing times are after the detection of the abnormalities) according to the Distributed generation sizes

DR size	Frequency Range (Hz)	Clearing time (s)
<30kW	>60.5	0.16
	<59.3	0.16
>30kW	>60.5	0.16
	< {59.8-57.0}	Adjustable 0.16-300
	<57.0	0.16

- Harmonics, it is an unwanted thing in any utility line because of its effects on the line and at the consumer end. The maximum THD permitted is 5% and other allowable content is mentioned in the table 2.4

TABLE 2.4 Maximum harmonic content for individual harmonic

Individual harmonics	N<11	11≤N≤15	17≤N≤21	21≤N≤33	33≤N
Allowed THD	4	2	1.5	0.6	0.3

- Flicker, IEEE standard does not allow the presence of flicker, but other standards such as the IEC has specific limits in terms of their irritability.

- Power factor, Standards require the power factor to be greater than 0.85 (lead or lag) when the load is larger than 10% of the rated power.

Reconnection of the inverter to the utility line is only possible if these regulations are abided by. The limitations on the voltage, frequency, harmonics and power factor are mentioned above and only if the grid-tied inverter abides these specifications the inverter is allowed to reconnect to the system. For example, if the inverter ceases to power the utility grid and does not follow the anti-islanding feature the PV system still powers the local loads and hence can be catastrophic if you try to fix anything before the PCC.

2.5. Summary

This chapter encapsulates the idea and guidelines for PV inverter grid-tie systems. The need for defining standards for grid-tie systems is a must; not only this, there is a need to develop a framework where these inverters can be tested for grid interconnection. Different inverter topologies have various control and functioning loops, hence the feedbacks from these tests might be helpful in giving insight to modelling problems. The presence of this chapter was to dive into the world of standards and specifications for any inverter model capable of connecting to the grid.

CHAPTER 3 : THEORETICAL ASPECTS OF DQ-FRAME

Chapter 3 explains the system that we are working on and what type of simulation software we use to model our system and analyze the harmonic content. This chapter also includes the distribution system and the type of inverters used. As discussed in the previous section, this can be one of the several inverter control architectures which can be studied extensively by the grid interconnection tests and their performance can be evaluated.

3.1. Single-phase Inverter Power Stage Modeling Based on Synchronous Reference Frame

Due to the limitation of having only one available phase in single-phase converters, the d-q synchronous frame transformation method is not readily adaptable to the single phase inverter unless a second orthogonal phase is created for every state variable in the circuit. The approach adopted here is a technique to create an imaginary orthogonal phase by generating a phase shift of 90degrees with respect to the real phase as shown in Figure 3.1.

These imaginary circuits will provide us with the basis for the formation of the PV inverter system architecture in DQ domain. Figure 3.1 gives an idea about the imaginary circuits for the PV inverter system, we can create our state space models using these circuits.
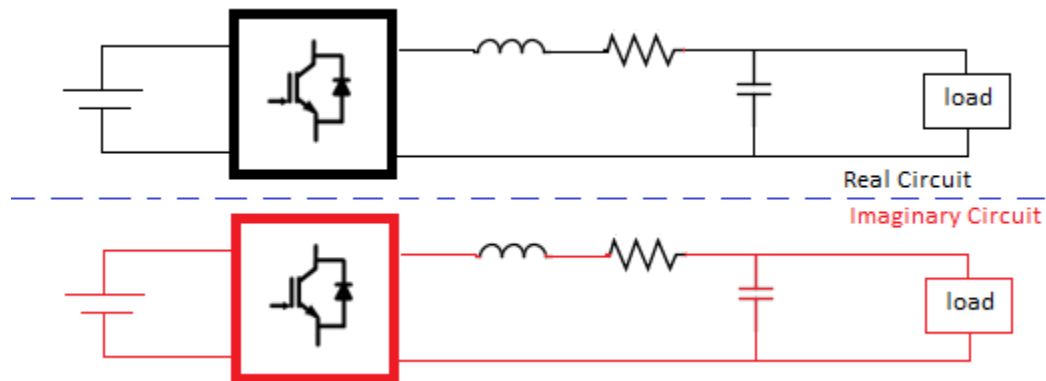
FIGURE 3.1: Real and Imaginary Circuit of the inverter

The real imaginary component concept is important as it will help us construct our transfer function of the inverter grid system and also building the dq-controller architecture.

Before that the linear model of the inverter and its state space equations can be defined using its differential equations obtained from the stand alone inverter circuit.

$$L\frac{di_l}{dt} + R_l i_l = V_{ab}u(t) - V_o \quad (3.1)$$

$$i_l = c\frac{dv_c}{dt} + \frac{V_o}{Z} \quad (3.2)$$

$$u(t) = \begin{cases} 1 & V_{ab} = V_{dc} \\ 0 & V_{ab} = 0 \\ 1 & V_{ab} = -V_{dc} \end{cases} \quad (3.3)$$

A single-phase inverter average circuit model was developed by splitting the inverter model into two 'virtual' circuits as shown in figure 3.2. The imaginary circuit has a set of 'virtual' components with the exact same values as those in the real circuit, here R and I components are the real and imaginary components or αβ components.
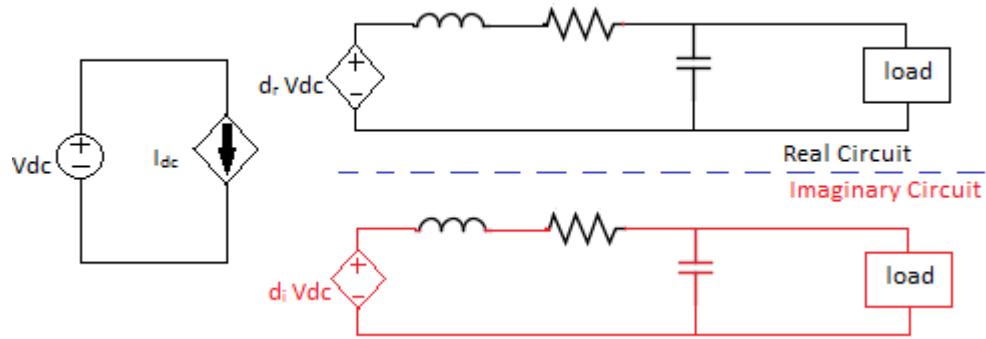
FIGURE 3.2: Average model of a single phase full-bridge inverter

State space equations for inductor current and capacitor voltage can be written after some simple mathematical analysis as followed:

$$L\frac{di_{l\_R}}{dt} + R_{l\_R}i_{l\_R} - V_{ab}u_R(t) + V_R = 0 \quad (3.4)$$

$$L\frac{di_{l\_I}}{dt} + R_{l\_I}i_{l\_I} - V_{ab}u_I(t) + V_I = 0 \quad (3.5)$$

$$i_{l\_R} = c\frac{dv_{c\_R}}{dt} + \frac{V_R}{Z} \quad (3.6)$$

$$i_{l_I} = c\frac{dv_{c_I}}{dt} + \frac{V_I}{Z} \quad (3.7)$$

$$\frac{d}{dt}\begin{bmatrix} i_{l\_R}(t) \\ i_{l\_I}(t) \end{bmatrix} = \frac{V_{ab}}{L}\begin{bmatrix} u_R(t) \\ u_I(t) \end{bmatrix} - \begin{bmatrix} i_{l_R}(t) \\ i_{l_I}(t) \end{bmatrix}\frac{1}{L}(R_l + Z) - \begin{bmatrix} v_{c_R}(t) \\ v_{c_I}(t) \end{bmatrix}\frac{1}{L} \quad (3.8)$$

$$\frac{d}{dt}\begin{bmatrix} v_{c\_R}(t) \\ v_{c\_I}(t) \end{bmatrix} = \begin{bmatrix} i_{l\_R}(t) \\ i_{l\_I}(t) \end{bmatrix}\frac{1}{C} - \begin{bmatrix} v_{cR}(t) \\ v_{cI}(t) \end{bmatrix}\frac{1}{CZ} \quad (3.9)$$

Averaging is done base on the assumption that the switching frequency is high enough to make the system dynamics almost constant for one period of switching frequency.

$$\frac{d}{dt}\begin{bmatrix} \overline{I}_{l\_R} \\ \overline{I}_{l\_I}(t) \end{bmatrix} = \frac{V_{dc}}{L}\begin{bmatrix} \overline{d}_R \\ \overline{d}_I \end{bmatrix} - \begin{bmatrix} \overline{I}_{l_R} \\ \overline{I}_{l_I} \end{bmatrix}\frac{1}{L}(R_l + Z) - \begin{bmatrix} \overline{V}_{c_R} \\ \overline{V}_{c_I} \end{bmatrix}\frac{1}{L} \quad (3.9)$$

$$\frac{d}{dt}\begin{bmatrix} \overline{V}_{cR}(t) \\ \overline{V}_{cI}(t) \end{bmatrix} = \begin{bmatrix} \overline{I}_{l\_R} \\ \overline{I}_{l\_I} \end{bmatrix}\frac{1}{C} - \begin{bmatrix} \overline{V}_{cR} \\ \overline{V}_{cI} \end{bmatrix}\frac{1}{CZ} \quad (3.10)$$

at the average input voltage to the filter is obtained as such:

$$\overline{u}(t)v_{ab} = \frac{1}{T}\int_{t-T}^{t} u(\tau)\, d\tau \rightarrow \overline{d}(t)V_{dc} \quad (3.11)$$

where d(t) is the average sinusoidal duty cycle of the inverter.

DQ model of the inverter can be developed after the average model has been developed. State space equations of the inverter and transformation matrices are already evaluated and are used to attain DQ equations which describes the inverter. Rewriting and using transformation matrix given below denoted here by T^{-1},

$$\begin{bmatrix} X_d \\ X_q \end{bmatrix} = T\begin{bmatrix} X_R \\ X_I \end{bmatrix} or \begin{bmatrix} X_\alpha \\ X_\beta \end{bmatrix} \quad (3.12)$$

$$\begin{bmatrix} X_R \\ X_I \end{bmatrix} or \begin{bmatrix} X_\alpha \\ X_\beta \end{bmatrix} = T^{-1}\begin{bmatrix} X_d \\ X_q \end{bmatrix} \quad (3.13)$$

$$T = \begin{bmatrix} cos\omega t & sin\omega t \\ -sin\omega t & cos\omega t \end{bmatrix} \quad (3.14)$$

$$T^{-1} = \begin{bmatrix} cos\omega t & sin\omega t \\ -sin\omega t & cos\omega t \end{bmatrix} \quad (3.15)$$

Applying the transformation matrix to the state space equation we can obtain the dq components. These are given by 3.16 and 3.17.

$$\frac{d}{dt}\left(T^{-1}\begin{bmatrix}\bar{I}_d\\\bar{I}_q\end{bmatrix}\right)=-T^{-1}\begin{bmatrix}\bar{V}_d\\\bar{V}_q\end{bmatrix}\frac{1}{L}-T^{-1}\begin{bmatrix}\bar{I}_d\\\bar{I}_q\end{bmatrix}\frac{1}{L}(R_l+Z)+T^{-1}\begin{bmatrix}\bar{d}_d\\\bar{d}_q\end{bmatrix}\frac{\bar{V}_{dc}}{L} \quad (3.16)$$

$$\frac{d}{dt}(T^{-1}\begin{bmatrix}\bar{V}_{dc}\\\bar{V}_{qc}\end{bmatrix})=T^{-1}\begin{bmatrix}\bar{I}_d\\\bar{I}_q\end{bmatrix}\frac{1}{C}-T^{-1}\begin{bmatrix}\bar{V}_{dc}\\\bar{I}_{qc}\end{bmatrix}\frac{1}{CZ} \quad (3.17)$$

By applying the chain rule to the $\frac{d}{dt}\left(T^{-1}\begin{bmatrix}X_d\\X_q\end{bmatrix}\right)$ in the equations above and

separating the dq components, the state space equation in the dq domain obtained. 3.19

and 3.20 show these equations.

$$T\frac{d}{dt}T^{-1}=\omega\begin{bmatrix}0 & -1\\1 & 0\end{bmatrix}=\begin{bmatrix}0 & -\omega\\\omega & 0\end{bmatrix} \quad (3.18)$$

$$\frac{d}{dt}\left(\begin{bmatrix}I_d\\I_q\end{bmatrix}\right)=\begin{bmatrix}D_d\\D_q\end{bmatrix}\frac{V_{dc}}{L}+\begin{bmatrix}0 & -\omega\\\omega & 0\end{bmatrix}\begin{bmatrix}I_d\\I_q\end{bmatrix}-\begin{bmatrix}I_d\\I_q\end{bmatrix}\frac{1}{L}(R_l+Z)-\begin{bmatrix}I_d\\I_q\end{bmatrix}\frac{1}{L} \quad (3.19)$$

$$\frac{d}{dt}\begin{bmatrix}V_d\\V_q\end{bmatrix}=\begin{bmatrix}I_d\\I_q\end{bmatrix}\frac{1}{C}-\begin{bmatrix}V_d\\V_q\end{bmatrix}\frac{1}{CZ}+\begin{bmatrix}0 & -\omega\\\omega & 0\end{bmatrix}\begin{bmatrix}V_d\\V_q\end{bmatrix} \quad (3.20)$$

3.2. DQ controller structure

DQ controller can be designed now that the DQ model of the single phase inverter

is obtained in equations 3.19 and 3.20. Controller consists of two channels, one for D and

one for Q, and each channel contains compensators for voltage and current loops. The

single-phase inverter closed-loop models and controller structure have adopted the inverter

model in the synchronous rotating reference frame. The continuous-time state space

equations for the inverter in the dq-domain can be written as:

$$u_d=L\frac{di_d}{dt}-\omega L i_q+r_l i_d+v_d \quad (3.21)$$

$$u_q = L\frac{di_q}{dt} + \omega L i_d + r_l i_q + v_q \quad (3.22)$$

The coupling terms in (derived from inverter modelling in the synchronous rotating reference frame) are decoupled for the controller. This is shown by the equation the figure 3.3.
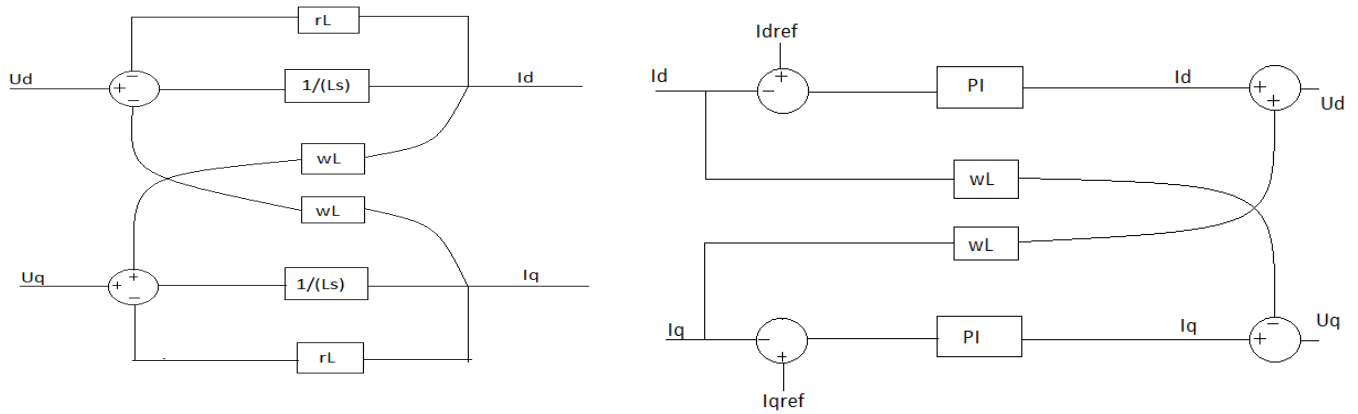

FIGURE 3.3: dq coupling terms on the inverter side and dq coupling terms on the control side

$$u_d = L\frac{di_d}{dt} + \omega L i_q + r_l i_d + v_d \quad (3.23)$$

$$u_q = L\frac{di_q}{dt} - \omega L i_d + r_l i_q + v_q \quad (3.24)$$

Where u$_d$ and u$_q$ are the control signals. V$_d$ and V$_q$ are the inverter output voltage components in the d-q frame respectively. The references I$_{dref}$ and I$_{qref}$ are acquired from the outer loop control.

- Outer loop based on Vdc control:

The proposed control strategy is intended to improve the power transfer and maintenance of array maximum power flow between inverter front-end and the inverter supplying the grid. This is achieved by using a feed-forward controller to control the dc-

link voltage by generating an appropriate d-axis reference current (Idref). Current

supplied to the grid via the inverter tracks the reference current Id-ref. The reference

current is determined by giving the difference between the DC-link voltage reference

Vdc_ref and the measured DC-link voltage to a PI controller. The feed-forward controller

is evident in the following blocks diagram of Figure 3.4
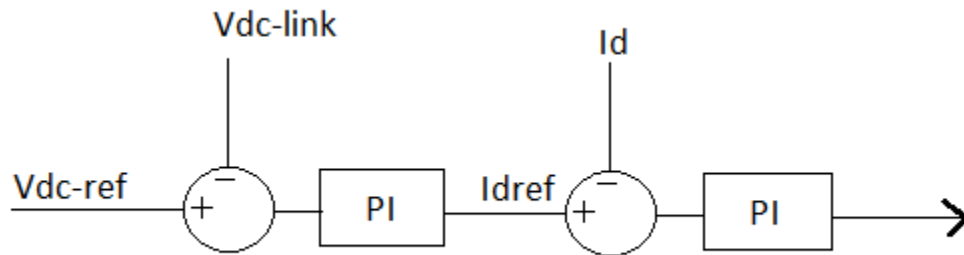
FIGURE 3.4: DC-link control loop

- Outer loop based on Active power control

In the rotating reference frame, v_q equals to zero when the rotating reference

frame is synchronized with the grid voltage then P and Q can be obtained by,

$$P = \frac{1}{2}(v_d i_d + v_q i_q) = \frac{1}{2}(v_d i_d) \quad (3.25)$$

$$Q = \frac{1}{2}(v_d i_q + v_q i_d) = \frac{1}{2}(v_d i_q) \quad (3.26)$$

In order to guarantee the all maximum power is transferred to the grid, the d-axis

current or active power command (i_{dref}) is proposed in the equations below. To control

the reactive power, the q-axis current or reactive power command (i_{qref}) is obtained in,

$$i_{dref} = \frac{2P}{v_d} = \frac{2P_{pv}}{v_d} \rightarrow \frac{2P_{max}}{v_d}; \ i_{qref} = \frac{2Q}{v_d} \quad (3.27)$$

3.3. Kp and Ki Values for the PI Controller

The single-phase voltage-source inverter and the grid are modelled in the synchronous rotating reference frame as two voltage sources. The continuous-time state space equation in dq-frame is given by 3.28 and 3.29.

$$u_d(t) = L\frac{di_d(t)}{dt} - \omega L i_q(t) + R i_d(t) + e_d(t) \quad (3.28)$$

$$u_q(t) = L\frac{di_q(t)}{dt} + \omega L i_d(t) + R i_q(t) + e_q(t) \quad (3.29)$$

Where $u_d(t)$ and $u_q(t)$ are the control signal components in the dq-frame respectively; $e_d(t)$ and $e_q(t)$ are the grid voltage; R is the equivalent line resistance and L is the equivalent line inductance. To model the closed loop system, the grid-tied model is represented as a state equation.

The discrete time model is represented by:

$$u_{d,k} = L\frac{i_{d,k}-i_{d,k-1}}{Ts} - \omega L\frac{i_{q,k}+i_{q,k-1}}{2} + R\frac{i_{d,k}+i_{d,k-1}}{2} + e_{d,k-1} \quad (3.30)$$

$$u_{q,k} = L\frac{i_{q,k}-i_{q,k-1}}{Ts} + \omega L\frac{i_{d,k}+i_{d,k-1}}{2} + R\frac{i_{q,k}+i_{q,k-1}}{2} + e_{q,k-1} \quad (3.31)$$

Assuming within one sampling interval, the current at the consecutive sample intervals are constant.

$$i_{d,k} \cong i^*_{d,k-1} \quad (3.32)$$

$$i_{q,k} \cong i^*_{q,k-1} \quad (3.33)$$

The steady state error can be looked at as the sum of all the previous errors,

$$u_{d,k+1} = \left[\frac{L}{Ts} + \frac{R}{2}\right]\left(i^*_{d,k} - i_{d,k}\right) - \omega L\left(\frac{i_{q,k} + i_{q,k-1}}{2}\right) + Ri_{d,k} + e_{d,k} \quad (3.34)$$

$$u_{q,k+1} = \left[\frac{L}{Ts} + \frac{R}{2}\right]\left(i^*_{q,k} - i_{q,k}\right) + \omega L\left(\frac{i_{d,k}+i_{d,k-1}}{2}\right) + Ri_{q,k} + e_{q,k} \quad (3.35)$$

$$u_{d,k+1} = K_p\left\{\left(i^*_{d,k} - i_{d,k}\right) + \frac{1}{T_i}\sum_{m=0}^{k-1}\left[i^*_{d,k}(m) - i_d(m)\right]\right\} - K_c\left(\frac{i_{q,k} + i_{q,k-1}}{2}\right)$$

$$+ e_{d,k} \quad\quad (3.36)$$

$$u_{q,k+1} = K_p\left\{\left(i^*_{q,k} - i_{q,k}\right) + \frac{1}{T_i}\sum_{m=0}^{k-1}\left[i^*_{q,k}(m) - i_q(m)\right]\right\} + K_c\left(\frac{i_{d,k} + i_{d,k-1}}{2}\right)$$

$$+ e_{q,k} \quad\quad (3.37)$$

Where,

$$Kp = \frac{L}{Ts} + \frac{R}{2}; \quad Kc = \omega L; \quad Ti = \frac{R}{\frac{L}{Ts} + \frac{R}{2}}$$

TABLE 3.1 PI values used for simulation purposes

Kp	Ti	Kc
0.02138	1	0.02

3.4. Per Unitized D-Q Control in RSCAD

The grid side values are normalized or per unitized before feeding into the dq control architecture. This helps in the development of the control in the hardware platform and also determining the Kp and Ki values for the PI.

The system has a power base of 1000 kW and voltage base of 230V on the secondary side of the transformer. The calculations for the other values are as follows,

$$Ibase = \frac{Sbase}{Vbase} = 4.348A \quad (3.38)$$

$$Zbase = \frac{Vbase}{Ibase} = 52.897\ ohm \quad (3.39)$$

$$Lbase = \frac{Zbase}{\omega base} = 0.14032 \quad (3.40)$$

The equations 3.38-3.40 are used to per unitized the control signals as shown in figure 3.5.
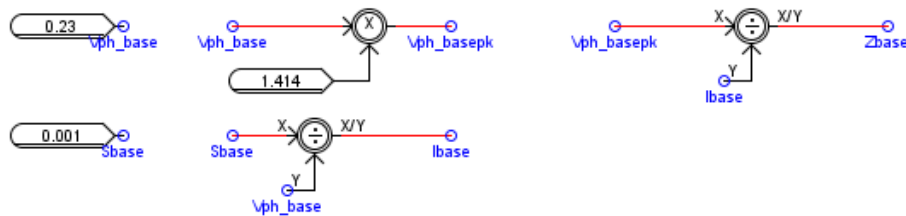
FIGURE 3.5 Per-unitization in RSCAD

3.5. Generation of the orthogonal signals

The limitation in our system is that it is a single phase system and we have only one phase available to us and adapting the d-q synchronous frame transformation becomes a task. So, if we want to create the additional orthogonal signal from the single phase inverter

signal, we need to trick the system. As already discussed, we use the technique of phase shifting the original wave by 90 degrees to generate the imaginary orthogonal signal and it is shown in fig 3.7. The imaginary orthogonal component is calculated or estimated from the actual component with a quarter cycle delay.
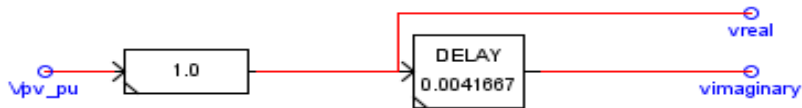
FIGURE 3.6: The delay block in RSCAD used for creating orthogonal signals

The delay blocks work very well for our system, and figure 3.7 shows the two components created in a single phase system. The real value was generated by a simple AC source; this was done to test out our logic for the orthogonal signal creation.
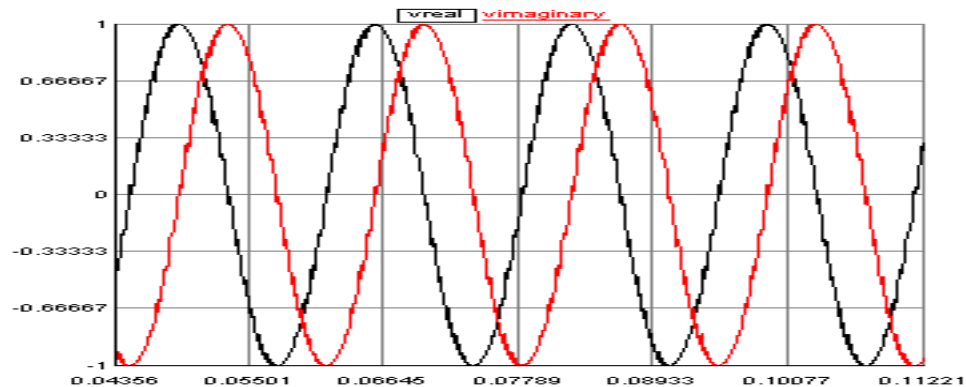
FIGURE 3.7: The real and imaginary components

3.6. D-Q Controller Structure in RSCAD

The controller architecture has already been designed and fig 3.8 and 3.9 shows the implementation of the same in RSCAD. The Kp and Ki values were calculated using equations 3.36 and 3.39 and the values are stated in the table 3.1.
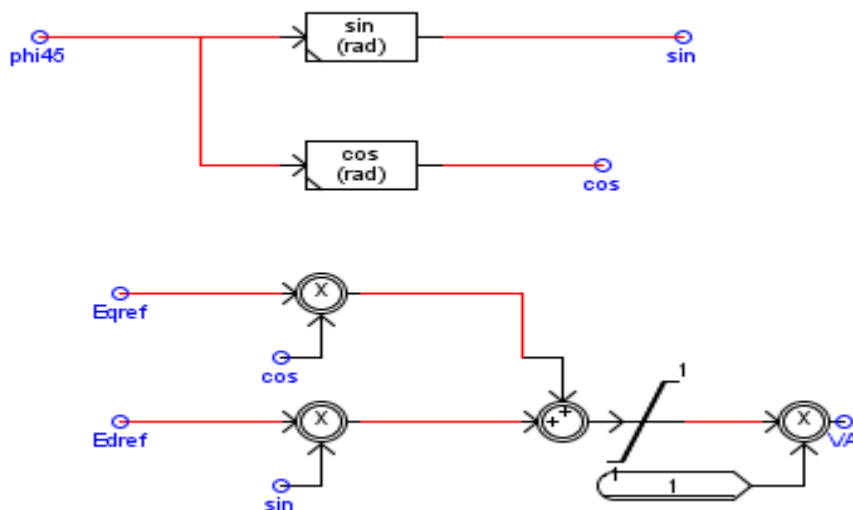
FIGURE 3.8: The controller structure (decoupled)
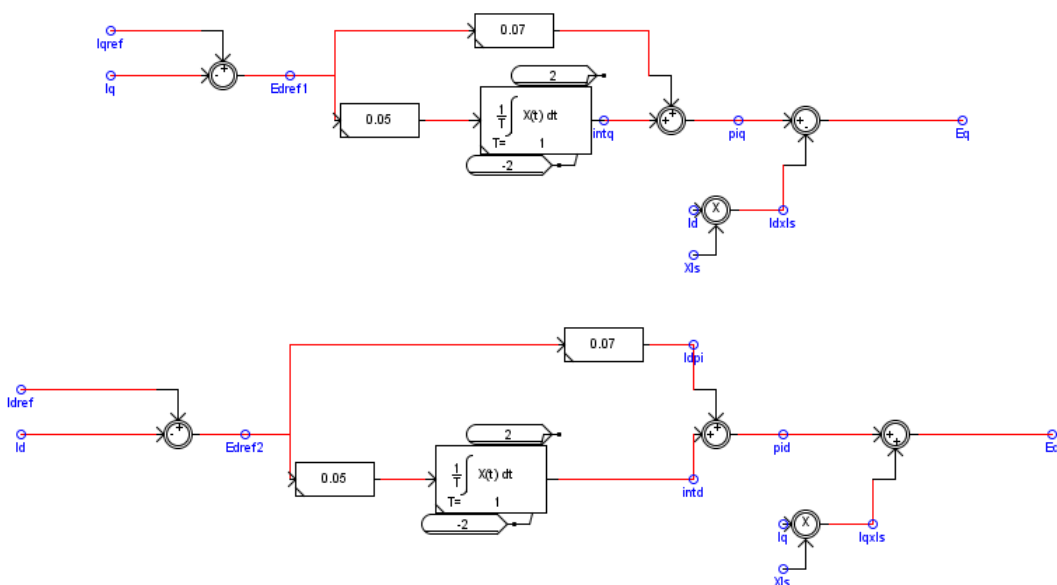
FIGURE 3.9: The voltage reference generation for the PWM using inverse park's transformation for single phase system

Here, the signals are from the per-unitized reference and post implementation of the orthogonal signal generation. The signals Ed and Eq are going to be converted back to the single phase system component by using the inverse park's transform for single phase as discussed in 3.1. The implementation in RSCAD is shown in fig 3.10.
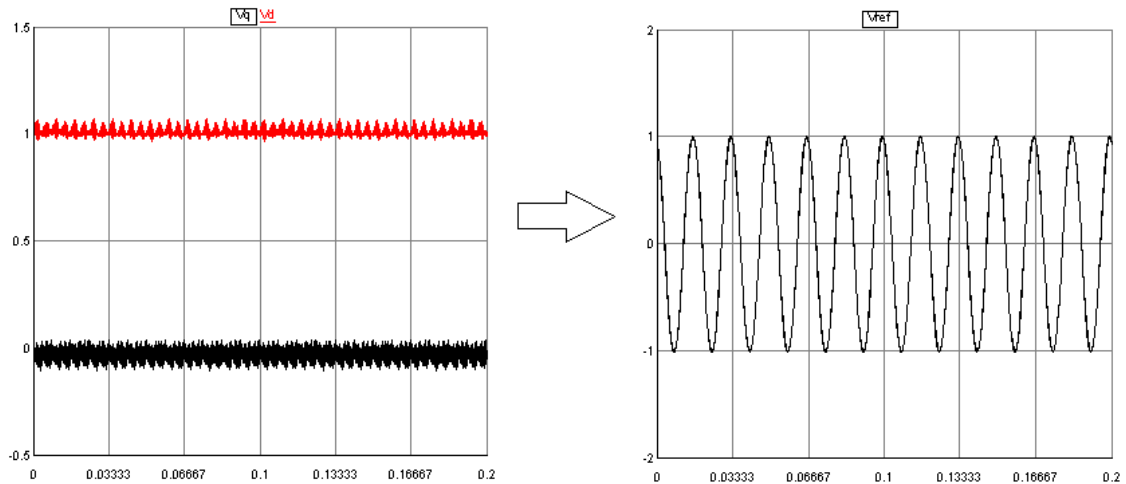
FIGURE 3.10: Vd and Vq transform to Vref or reference signal for the PWM

The graphs in figure 3.10 was generated using a simple AC source connected to a load. This was done to check our logic behind the dq- to single phase signal generation. We can verify with the above graph that this topology for generation of orthogonal signals can be used in our PV inverter system control.

3.7. Summary

This chapter proves that the generation of the orthogonal signals by phase shifting original signal by 90 degrees is an effective one. This helps us utilizing the d and q components of our currents for our inner current control loop. Not only this, the chapter dives in the theoretical aspects of the dq-frame inverter modelling and developing the controller structure required to decouple the two components.

CHAPTER 4 SYSTEM DESCRIPTION

Chapter 4 explains the system that we are working on and what type of simulation software we use to model our system and analyze the harmonic content. This chapter also includes the VP4 distribution system and how it was modelled mathematically for our simulation purposes. We look into the network and establish a lumped network with one rooftop PV inverter system.

4.1. Actual System Overview

Several governments worldwide promote the use of distributed power (DP) generation using renewables with subsidies and customer programs. This include offshore wind farms and several roof-mounted photovoltaic (PV) arrays are installed on most of the roofs of individual homes, apartments, and communal buildings. An example of such an endeavor is the Dutch Nieuwland Project, near Amersfoort, The Netherlands, where in total, 12000 m PV arrays were installed, on 500 homes. In total, renewable energy of 1-GWh p.a. is generated by this project. The distribution system we are using is a part of a big distribution system in the Netherlands known as the Vernormeer network. We have chosen a part of the distribution network which is the VP4 network, where we have 36 homes out of which 18 homes have roof mounted PVs which produce 1kW of power per house. The individual homes with roof mounted PV arrays are connected on three 400-V network sections, each supplied from a separate 10-kV/400-V transformer. Different types of PV inverters are currently installed on this network

All the homes are modeled as a 300W load, the capacitances of the houses without an inverter were modeled to be 3uF and with the inverter as 9uF. The homes with similar characteristics were lumped as a single model. Figure 1.1 shows the VP4 network and the impedance modeling of individual houses.
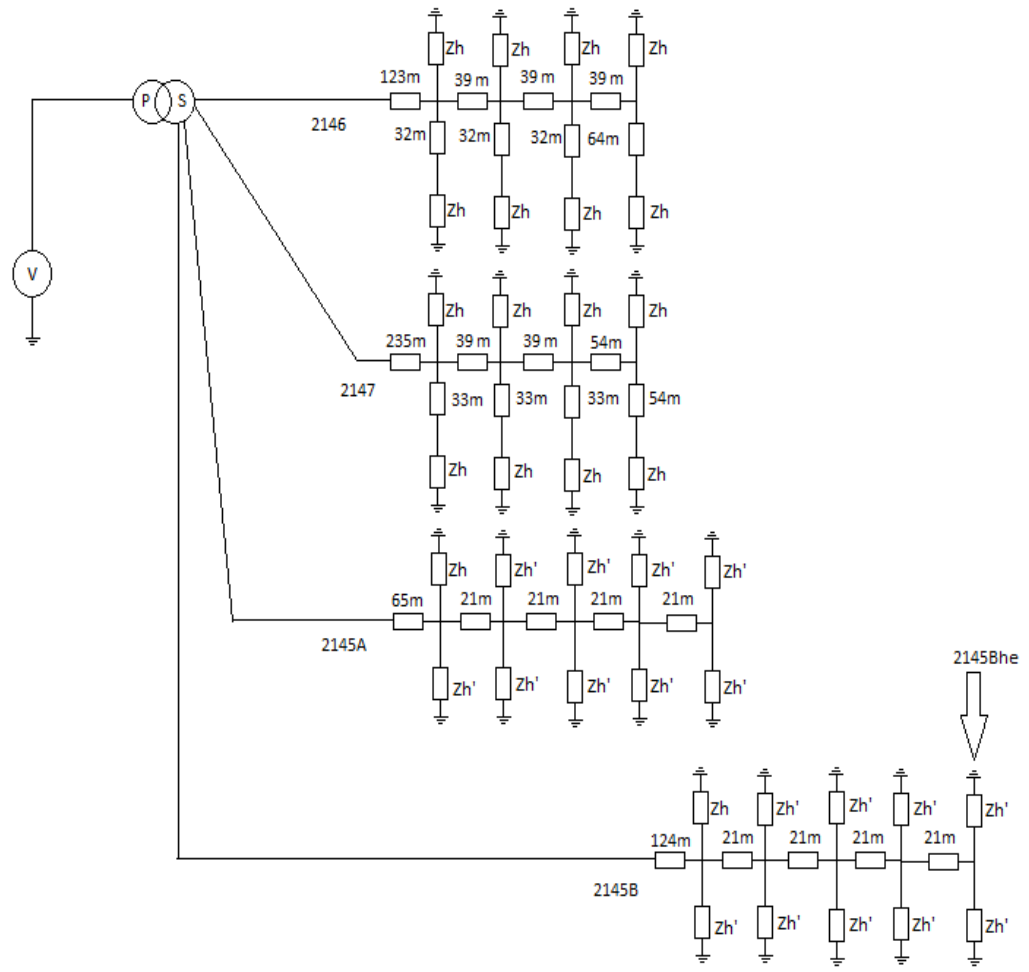

FIGURE 4.1 Model VP4 network with PV inverters

Measurements in these Dutch network showed that in high penetration of PV generation, the inverters under certain circumstances switched off abruptly. This might be due because of the power quality standards not maintained at the point of common coupling

(PCC). This might be the case even when all the PV inverters individually satisfy the IEC 61000-3-2 specification. We can analyze these problems by using these measurements, setting up practical laboratory experiments and simulation. These data which are referred from [6], can be used to create our distribution network on RTDS and perform detailed analysis on real time and obtain possible solutions. RTDS is a useful tool through which we can integrate our hardware and our simulated system together, this process is known as hardware in loop (HIL).

4.2. System Modeling

Real time digital power system simulation (RTDS) software was used for our modeling and simulation. This tool is helpful to not only analyze the system in real time but also give us the luxury of doing HIL with real PVs and inverter installed on the hardware side. Firstly, we model the VP4 network on RTDS, before the modeling we need to understand the network and the measurement values which are reference in [6].

The distribution line modeling was done based on the mathematical calculation. The data for cables/LV lines were given as:

$$R = \frac{0.23}{1000} \frac{Ohm}{m}$$

$$Xl = \frac{0.078}{1000} \frac{Ohm}{m}$$

$$C = 420e^{-9} \frac{F}{Km}$$

The impedance calculation of the system is also done on the basis of the information provided by [6], we model our homes based on the active power and the capacitance provided and the houses are modeled as given in table 4.1

TABLE 4.1 Two types of houses in our system Zh (without PVs) and Zh' (with PVs)

House capacitance 3uF (Zh)	171.59-28.51j
House capacitance 9uF (Zh')	141.226-70.41j

After modeling our system according to Figure 4.1, we get a good idea of the impedances in the system. Now we lump the system to a simpler form so as to make it easier for us to verify the Power flow, current and voltage at each branch of the network. The Impedance diagram is shown in figure 4.2.
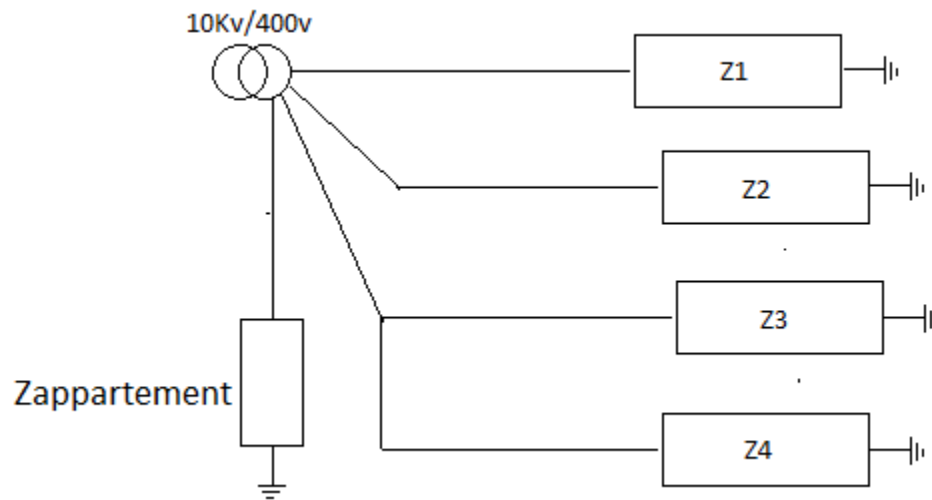

FIGURE 4.2: Impedance diagram for VP4 network

We have four branches as shown in Figure 4.1 and 4.2, where branches 1 and 2 have homes without rooftop PVs attached and branches 3 and 4 with the rooftop PVs. As mentioned before, houses with similar characteristics are lumped together. There is an additional line with one house (Zappartement) which we are excluding in our simulation for simplification purposes.

TABLE 4.2 Impedances and Currents of the branches in VP4 network

Branch number	Impedance	Current
2146	21.48-3.55j	10.423+1.723j
2147	21.50-3.55j	10.423+1.723j
2145A	17.1797-2.844j	13.03+2.1572j
2145B	17.198-2.84j	13.02+2.149j
appartement	17.174-2.847j	13.034+2.161j
I_{total}		59.93+9.9132j

The current values in the table is calculated under the assumption that there is no PV installation, this is done to simplify our math when we are calculating the power output and current of one house and matching it to that of [6].

The experimental evaluation that we will be doing is not for 18 rooftop PVs, but that for 2 rooftop PVs. This is done because the capability that we have on the hardware side is for a 2kW system i.e. 2 houses in the VP4 system. Therefore, we evaluate the math for the power and current on the PCC of one house first and then two houses. Here, we will have to fall back on our basics of Thevenin's theorem of circuits to isolate one house from the distribution system.

To analyze the behavior of one PV inverter tied to the grid we consider the impedance seen by the last house 2145Bhe or rather the impedance seen by the inverter mounted on that house. For that we consider formulating a thevenin's equivalent diagram of the circuit.

Case1: One house system
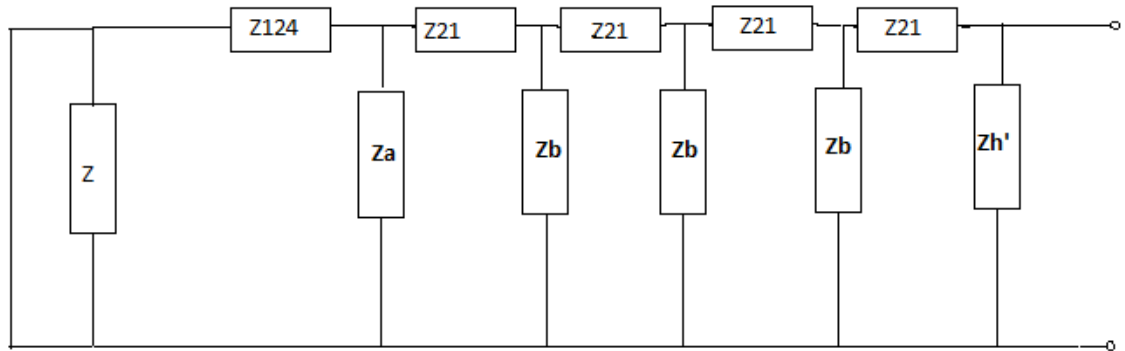
FIGURE 4.3 Thevenin equivalent circuit for 2145Bhe

The impedance Z is the combination of the first three branches of the VP4 network shown in figure 4.3. Za is the equivalent impedance of Zh and Zh' and Zb is the equivalent impedance of Zh' and Zh'. Here,

$$Z = Z1||Z2||Z3 = 4.77 - 0.79j \quad (4.1)$$

$$Za \approx Zb = 85.795 - 14.255j \quad (4.2)$$

Solving it, we get our thevenin's equivalent circuit as:

$$Zth = 0.0612 + 0.01613j \quad (4.3)$$

Zh consumes: Izh = 1.304+0.2167j or 1.322∠9.4   (4.4)
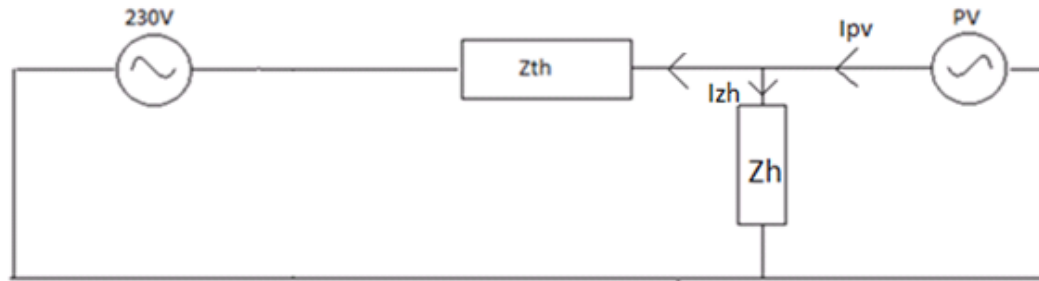
FIGURE 4.4 Thevenin equivalent circuit for one home (2145Bhe)

Current to the grid or at PCC (Ig):

4.225-1.227j or 4.4∠-18 A

Current from the inverter:

Ipv= (4.225-1.227j+Izh) =5.529-1.01j or 5.62∠-11 A   (4.5)

The voltage and current waveforms shown in figure 1.4 are the actual voltage and current seen on the house 2145Bhe. The current is out of phase with the voltage, this means that the PV is pushing the excessive power out. The Grid current shown in the figure is used to calculate the current from the PV and hence its power transfer capability can be known. To verify, we can now calculate the secondary transformer current now that we know our PV capability and the total current when the assumption of no PV was made in table 4.2.

According to our calculations the current flowing to the grid from our system will be:

Igrid= (Ipv*18)- Itotal   (4.6)

Where,

Ipv= 5.529-1.01j

Itotal= 59.93+9.9132j

Therefore, Isecondary= - (39.592-29.7312j) or 49.51∠143.09   (4.7)

The figure 4.5 shows us how accurate we are in our thevenin's model for the one house system connected to the VP4 distribution network. There is a minor error on the current, this is due to our exclusion of the Zappartement as stated initially.

TABLE 4.3 Comparison of data on the paper and our calculation

Data in the paper:

	Current A	Real	imag
Secondary	50∠140	-38.30	32.139j
2145	82.76∠162	-78.5	26.22j
2146&2147	10.60∠10	10.44	1.841j
Appartement	8.5∠48	5.69	6.32j

Our calculation:

	Current A	Real	imag
Secondary	49.51∠143.09	-11.766	21.6704j
2145	73.482∠160	-73.482	22.5j
2146&2147	10.60∠9.4	10.423	1.723j
Appartement	8.5∠48	13.034	2.161j

Case2: Two house system

Considering three houses to be analyzed and the impedance seen by them, we consider the following thevenin diagram in figure 4.5.
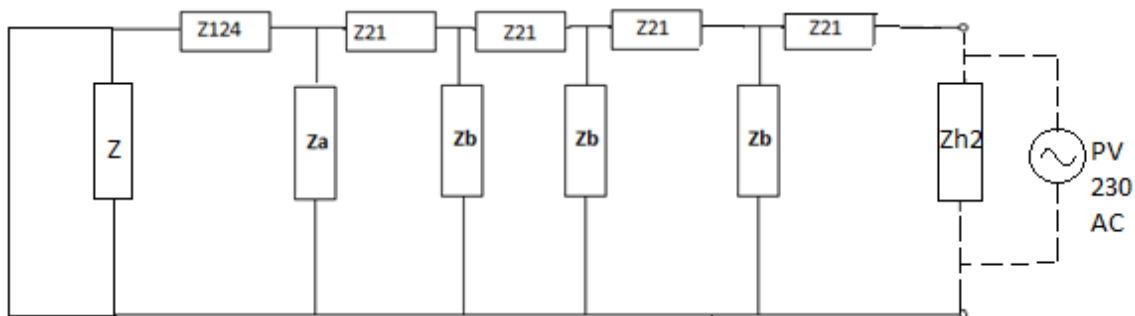
FIGURE 4.5 Thevenin circuit evaluation for 2 house system

Z is Z1||Z2||Z3 = 4.77-0.79j   (4.8)

Za= Zb= Zh||Zh = 85.795-14.255j Ohm   (4.9)

The impedance Z is the combination of the first three branches of the VP4 network shown in figure 4.5. Za is the equivalent impedance of Zh and Zh' and Zb is the equivalent impedance of Zh' and Zh'. Here, Zh2 is the denotation of the two houses.
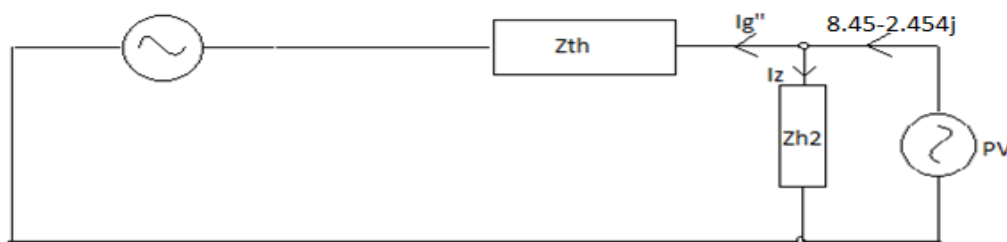
FIGURE 4.6 Thevenin equivalent for two house system

Where:

Zth= 0.0612+0.0162j Ohm   (4.10)

Iz= 2.61+0.4334j or 2.64∠9.44   (4.11)

Ig''= 8.45-2.454j   (4.12)

Ipv2= 11.058-2.02j or 11.24∠ − 10.35 (4.13)

4.3. System Modeling in RSCAD

The system mentioned in figure 1.1, was created in RSCAD and was tested connected to the utility without the PV installed on the house 2145 Bhe. Figure 4.7 shows the distribution model in RSCAD, the system is quite big so fig. 4.7 shows the first three branches of the network, this is simulated in the 2nd rack of the RTDS, the 3rd rack simulates the 4th branch including the 2145Bhe and the PV inverter system as shown in figure 4.8.

Figure 4.9 shows the modelling of 2 houses in RSCAD, this is shown because eventually these houses will be a point in the simulation taking data from an external signal coming from the real time data from the 2 house inverter set up in the UNC lab. The Distribution feeder is simulated in rack one and is shown in the figure 4.10.

The voltage regulator is needed on the feeder for several reasons, and in distribution networks voltage levels might deviate from the ratings which might be caused by:

- Load change and load power factor
- Tap position

The distributed generators such as the PV plants can cause voltage to rise and the purpose of the load tap changing (LTC) on the transformer is to mitigate severe effects that can cause the voltage change and hold the voltage at the desired level.
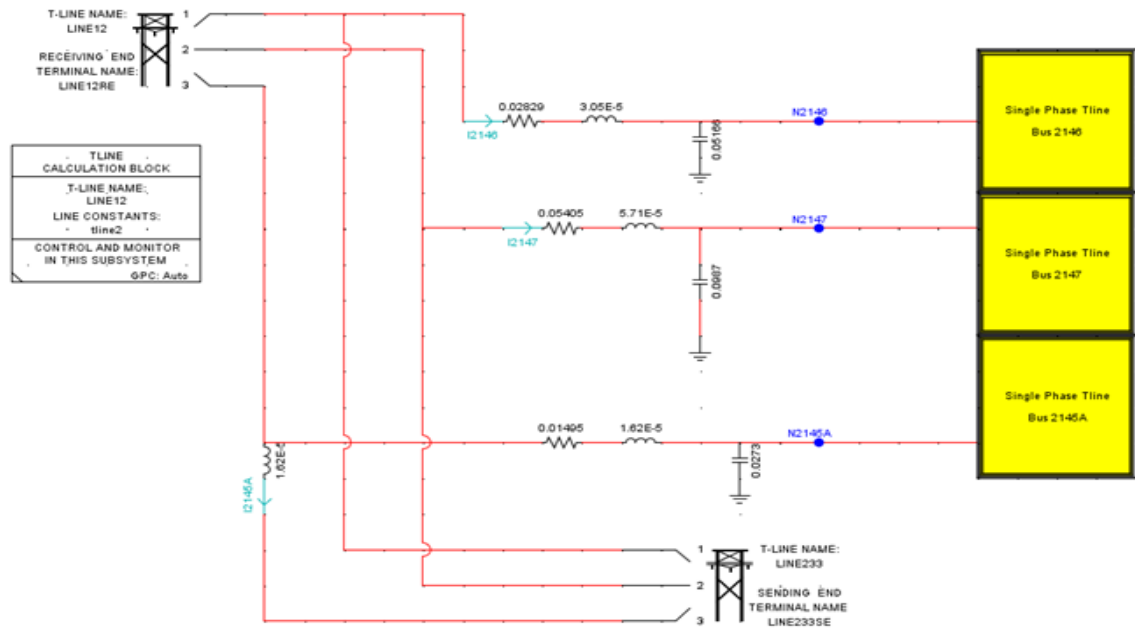

FIGURE 4.7: Distribution network of VP4 in RSCAD

The distributed generators such as the PV plants can cause voltage to rise and the purpose of the load tap changing (LTC) on the transformer is to mitigate severe effects that can cause the voltage change and hold the voltage at the desired level.

The functionality of the LTC are based on the following actions:

- The voltage set point, usually the single phase low voltage.

- Bandwidth, defining allowed band i.e. Vsetting$\pm$0.5*Bandwidth

- Time delay, in order to have buffer for short-term voltage fluctuations.
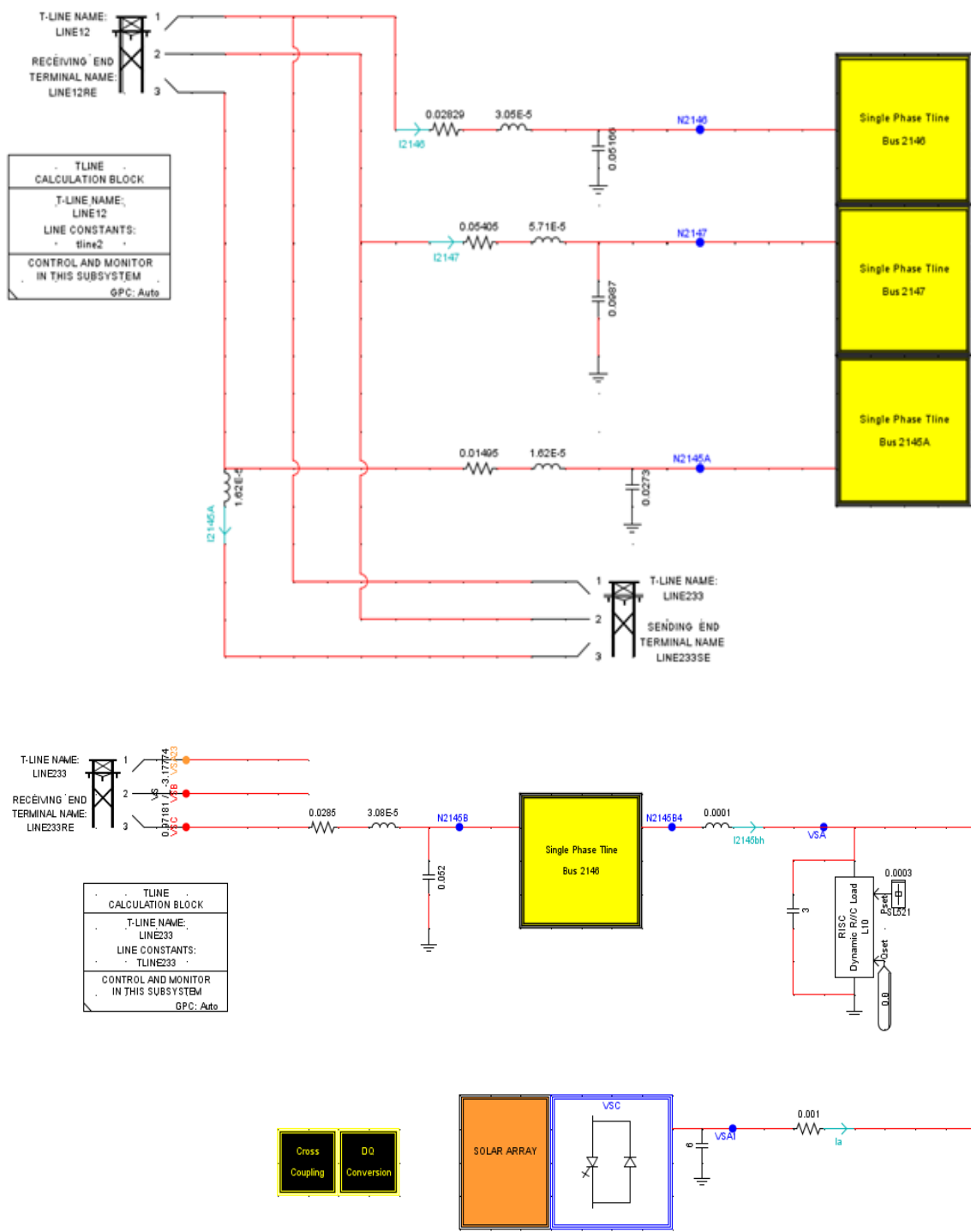
FIGURE 4.8: Distribution system on the 3rd rack (includes 2145B branch, PV and it control elements)
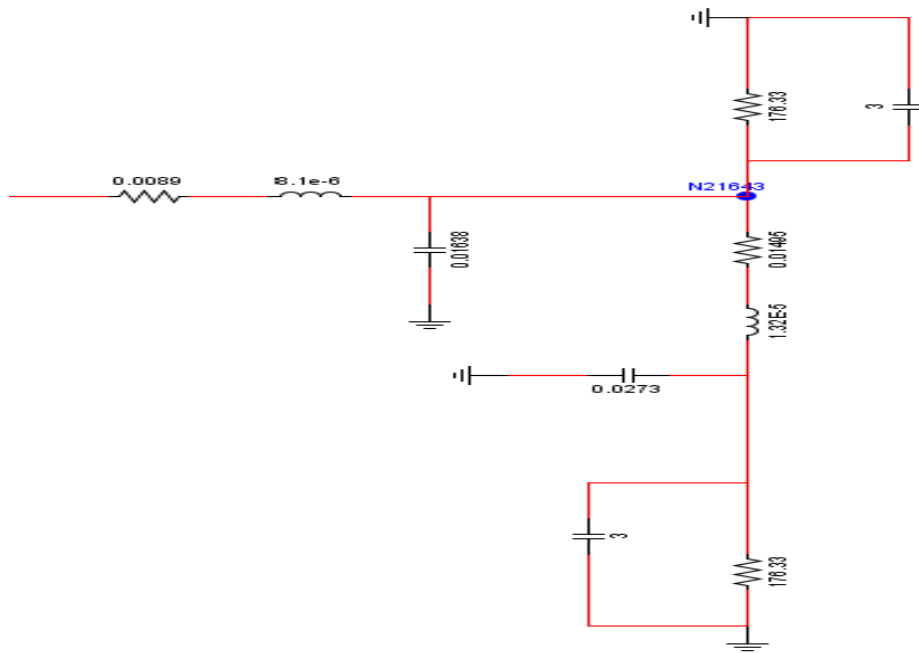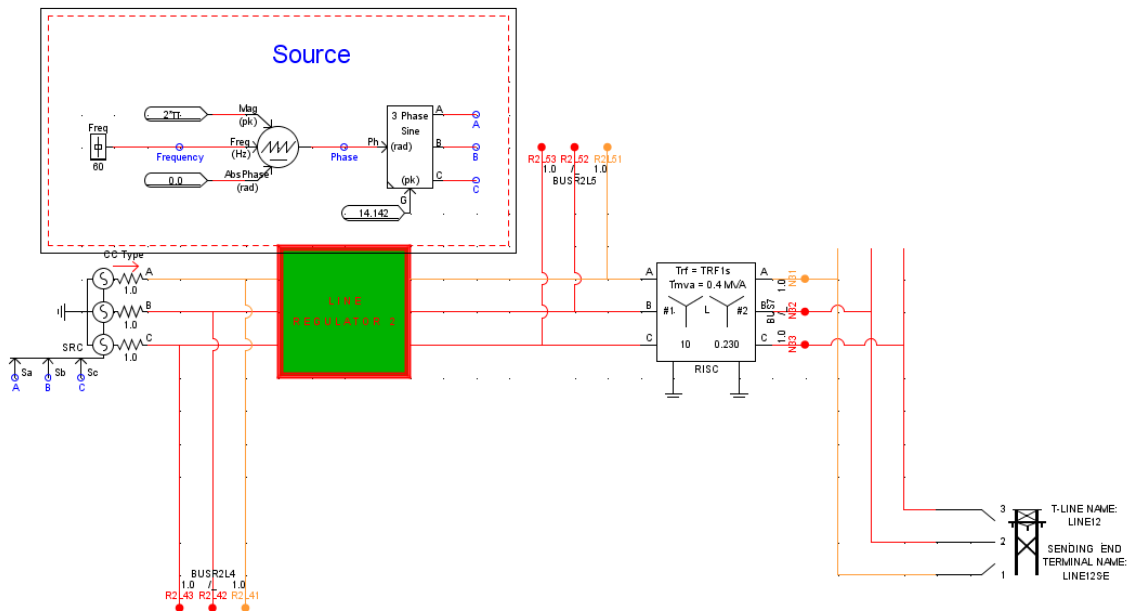
Figure 4.9 Model for 2 houses

Figure 4.10 Feeder on rack 1

4.4. Distribution System Simulation in RSCAD

The results for the power, voltage and current per branch and on the secondary transformer side are evaluated and compare with [6]. As stated in table 3.2 the currents in branches are:

- Branch 2147 and branch 2146 currents are 10.423+1.723j or 10.5645∠10.43 according to our calculations before. Figure 4.11, shows the branch current during our simulation in RTDS.
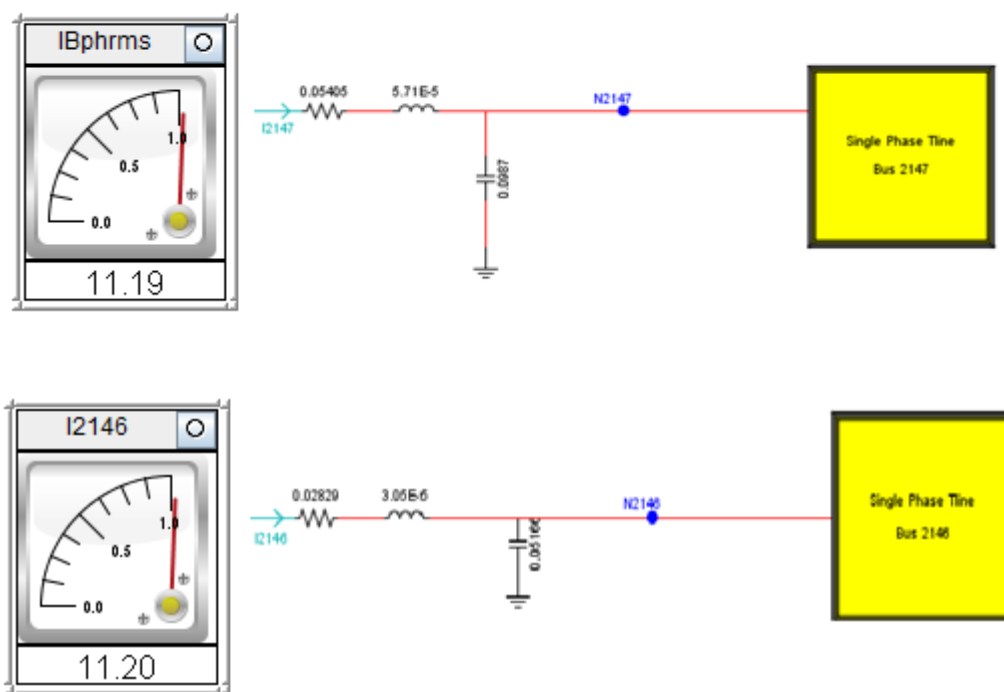
Figure 4.11: Branch 2147 and branch 2146 currents
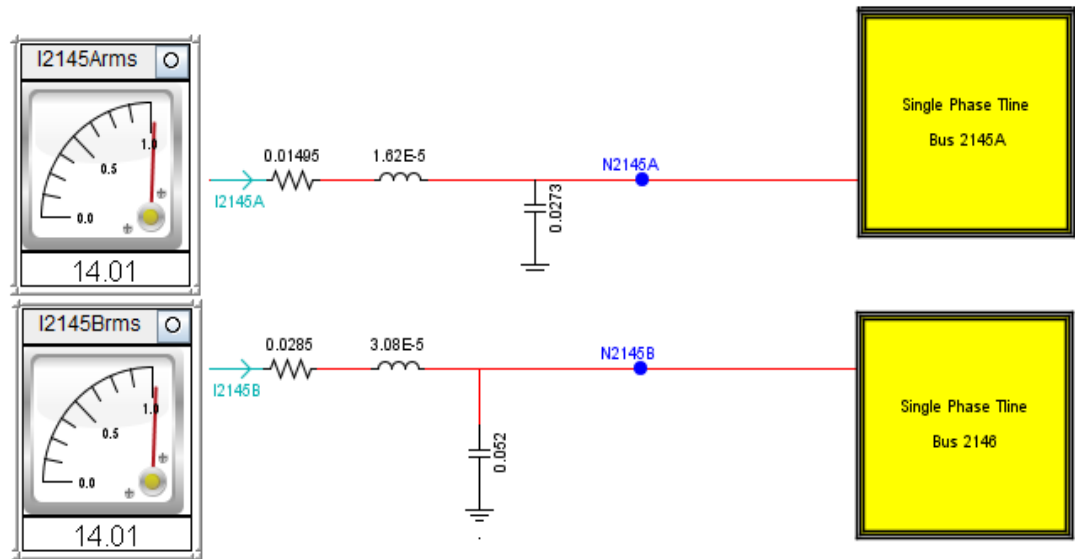
Figure 4.12: Branch 2145A and branch 2145B currents

- Branch 2145A and 2145B currents are 13.03+2.1572j or 13.207∠10.45 according to our calculations before. Figure 3.11, shows the branch current during our simulation in RTDS.

4.5. Hardware Implementation

The Hardware implementation was done for grid interconnection test and grid impedance matching. The main idea for our work was to have a test bed for future testing of power quality on increasing PV penetration and elimination methodologies. Table 4.1, describes the lab capability at UNC charlotte for inverter testing. RTDS has an advantage of simulating in real time and also hardware in loop (HIL) capabilities.

The inverter implemented for the hardware setup is rated for 1500VA, 230V output. The supply is from the TerraSAS PV simulator and its capability is mentioned in table 4.4.

This PV has the capability to be grid-tied, and was connected to the grid here at UNC charlotte and the IEEE1547 testing and grid impedance matching was performed. The generation of the anomaly was generated by a device called the Power Amplifier. The devices not only change the voltage and current, but it also has the capability to alter frequency and generate harmonics.

TABLE 4.4: Comparing the 2 cases for rooftop PVs and the capability of the PVs present in the Smart Grid lab UNC Charlotte.

houses	Current supplied By PV (amperes)	Current at PCC (Amperes)	Grid impedance (Ohms)	Power (VA)
1	5.62∠-11 A	4.4∠-18 A	0.0612+0.01613j	1292.6
2	11.24∠-10.35	8.45-2.454j	0.0612+0.0162j	2585.2
What we have (1 PV simulator)	Max voltage (Voltage)	Max current (current)		Max power DC
1	150V	5.6 A		840

Types of connections to be supplied by the programmable power, for which the IEC 61000-4 is defined for:

Class 1:

This class includes the supplies that involves the use of sensitive equipment which change abruptly for small disturbances in the power supply. For example, the devices and instruments in laboratories, computers, etc.

Note: Class 1 environments normally contain equipment, which requires protection by such apparatus as uninterruptible power supplies (UPS), filters, or surge suppressers.

Class 2:

This includes The PCCs and IPCs for consumer and industrial systems. They are systems with more heavy loads which are quite stable for a wide range of operations. The components are designed for application in industrial enviornments.

Class 3:

This class applies only to IPC's and has higher level of durability for disturbances in industrial environments. The devices in these configurations include:

- A major part of the load is fed through converters;
- Welding machines are present;
- Large motors are frequently started;
- Loads vary rapidly.

IEC 61000-4-11:

Test involves a series of voltage dips and variations that simulate real world conditions that may occur on AC power distribution networks. This test is to ensure a

product's immunity from such voltage anomalies. Voltage dips occur at zero-degree phase angles using different levels. Typical test levels are 0 %, 40 % and 70 % of the nominal test voltage. Voltage variations are performed at 40 % and 0 % of the nominal test voltage. These variations consist of specified voltage rise and fall times can be tested on an inverter and its performance can be evaluated.

Considering the Class 2 type of connection the already saved in file regarding IEC 61000-4-11 defined the voltage dips and variations as:

Dips:

1. Vac=0 for 0.5 cycles in an interval of 10 seconds

2. Vac=0 for 1 cycle in an interval of 10 seconds

3. Vac=84V for 30 cycles in an interval of 10 seconds

After 1 has occurred 2 and 3 are executed in the same flow with a gap of 10 seconds.

Variations:

Vac=0; fall time=0; cycle stay=1; cycle rise=30; cycle repeat=3; delay between repeat=10s

61000-4-14:

This test sequence includes a series of voltage changes that we can commonly observe in utility grids. The objective of this test is to test the immunity of a product from these anomalies.

Voltage fluctuations are applied at different levels for different product categories. The user must determine the product class and select the appropriate test level. During the test run, voltage changes are applied as specified by the selected test mode and for specified periods of time.

The test sequence can be programmed by setting the nominal voltage in %, the test level which is the change from the nominal voltage in %, the number of times each test level repeats (consecutive 5 second periods) and the delay between each set of test levels. Finally, each step in the sequence data grid can be repeated 1 or more times. (A Delay of 1 means the set it only run once.) The various columns in the test data setup are shown in the figure below.

This test is same for class 2 and 3 types of connections and have the following properties and procedures:

- Initially the voltage is at the nominal rating and is fluctuated ±12% as seen in the figure.
- Time between two fluctuations is 5 seconds and the immunity test goes on for 3 repeat cycles.
- The second part (which occurs after the first 3 iterations) occurs after a delay of 60 seconds.
- Second part involves the Vnom to drop to 90% of its value and the voltage is brought to +12% repeatedly from the 90% Vnom for 3 iterations and one iteration lasts for 5 seconds.

- After another 60 seconds delay the 3rd stage involves the Vnom to go to 110% of its value and fluctuate from that point to -12% with three iterations lasting for 5 seconds.

- Individual step detail is shown in figure 2.

Every fluctuation follows the 5 second hold time whereas the 60 second delay can be altered.

61000-4-28:

Most of the areas don't even notice frequency fluctuations, but areas where the grid tends to be smaller in size, for example islands, isolated grids etc. The frequency changes here are noticeable and cannot be ignored. Hence, there is a need for the equipment to be tested for frequency variations and test their durability to it.

The, IEC 61000-4-28 is a published standard. Its scope is the immunity testing of electrical and electronic equipment with a rated input current not greater than 16A per phase to variations in the power frequency. Evaluation based on long term variations are not considered in this test, because of the load size. This tests is for much smaller purposes, such as residential areas or smaller commercial sectors.

Figure 4.15 shows the testing program in the RS-90. These frequency variations were applied to our inverter and its performance was evaluated later. One thing should be noted that for our hardware testing we have used GFX series OUTBACK inverters and the testing are on a three phase system.
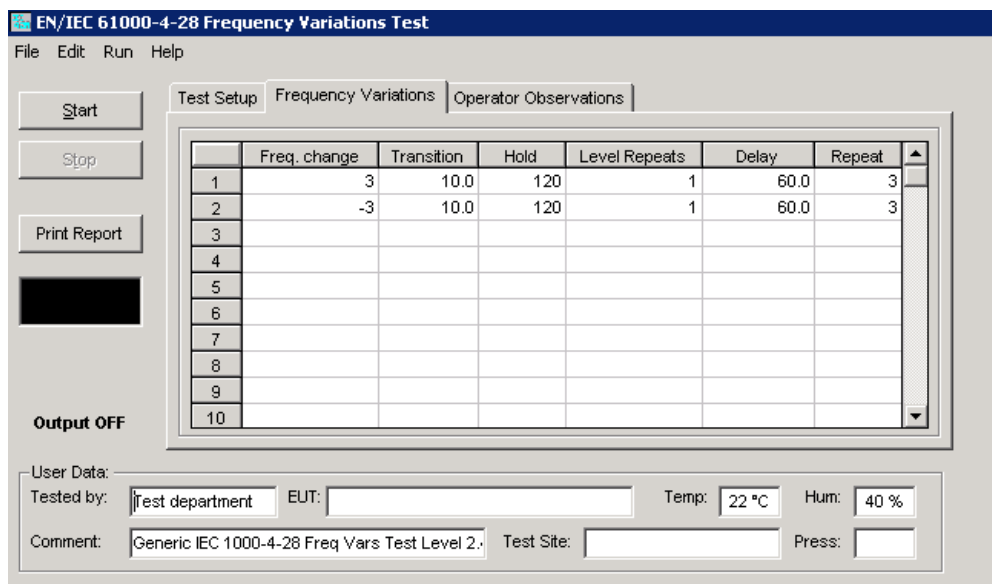
Figure 4.15: Frequency variation program in RS90

Test Implementation and Test Sequence:

The frequency variation is applied for a period of 120 seconds (Hold period) with a minimum of 60 seconds (Delay) between variations. Frequency switching occurs at the zero crossings for full compliance testing. The actual change from one frequency to another takes place over a period of time called the transition time (Trans.). The suggested transition time to be used is 10 seconds but the MXGui/RSGui supports transition times from 0 sec (instantaneous change) to 60 seconds. Each test level is repeated the number of times specified by the Level Repeats field value before the delay is applied.

To correctly follow the test draft, this field should be set to 1. The Repeat field is used to repeat the entire test step including the delay and should be set to 3 to meet the draft standard. The number of repeats, the transition time, the hold time and the time between repeats can be set as part of the test specification in the GUI. This allows changes to the test standard to be accommodated in the future. Important to note that using this

application in RS-90 software requires the user to click on the voltage regulation check which is strictly prohibited by the IEEE1547 as we will see later. Voltage fluctuations using RS-90 Programmable power according to IEEE 1547 specifications can be seen by,

Case 1:

Less than 50% of Vnom (here 42% of Vnom) for 3 seconds. For 3 seconds we are providing with an anomaly to the frequency which is greater than its time tolerance i.e. >0.16 seconds.
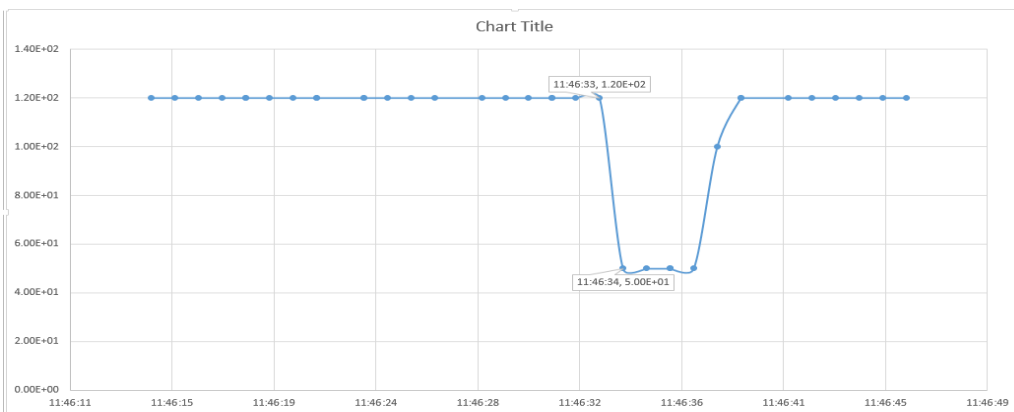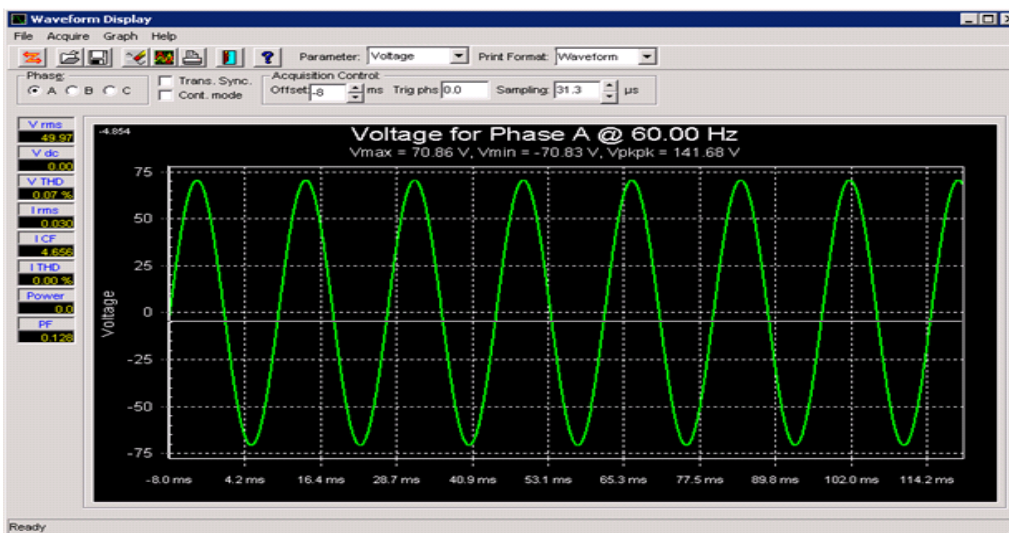

Figure 4.16: Voltage fluctuations provided by RS90 and the tripping behavior of the inverter (excel grpah)

for V<50% Vnominal

Case 2:

50%≤V<88% of Vnom for 3 seconds (here Vrms=84 which is 70% of Vnom)
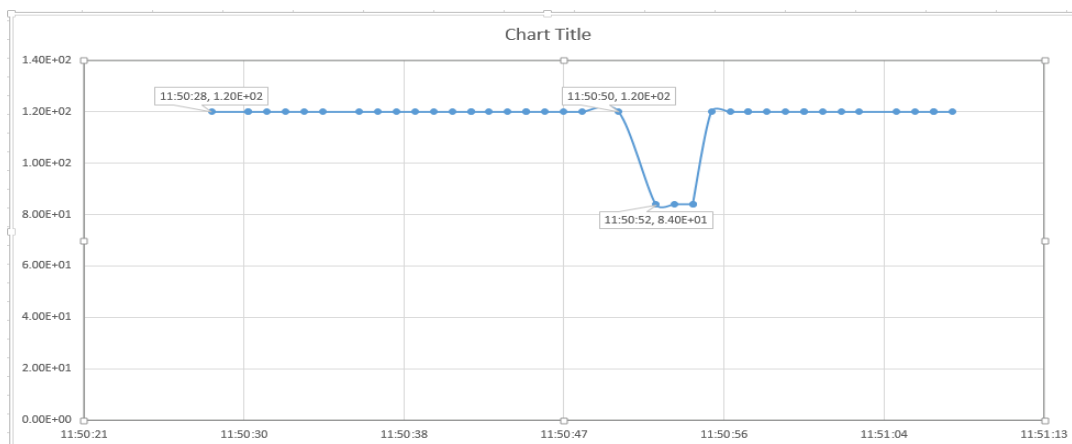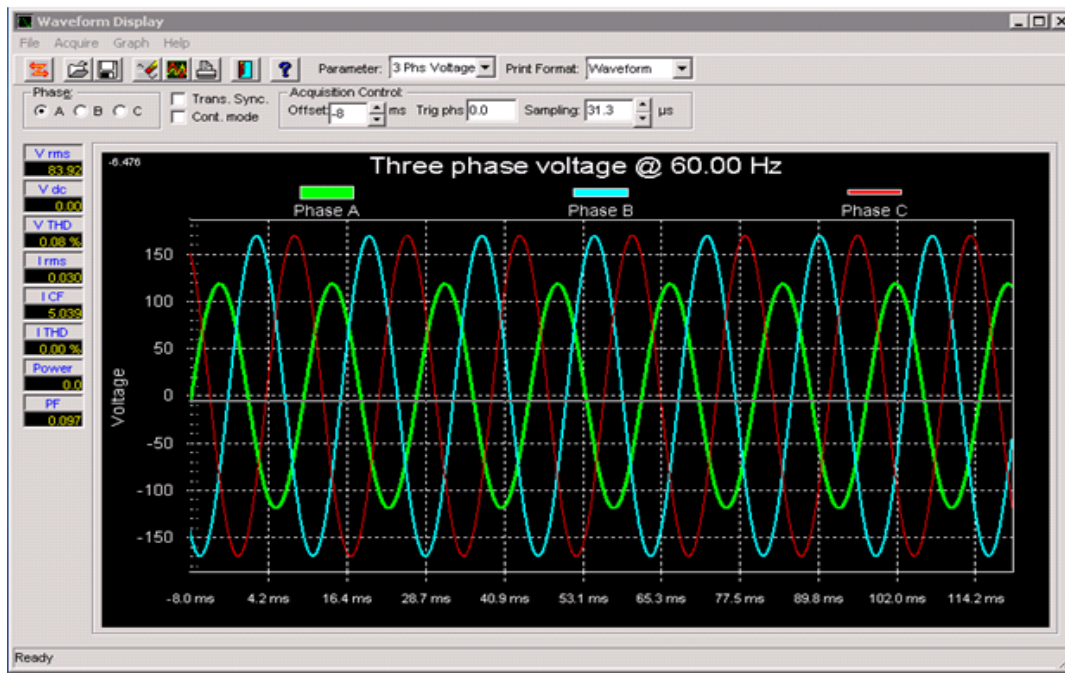
Figure 4.17: Voltage fluctuations provided by RS90 and the tripping behavior of the inverter (excel grpah)

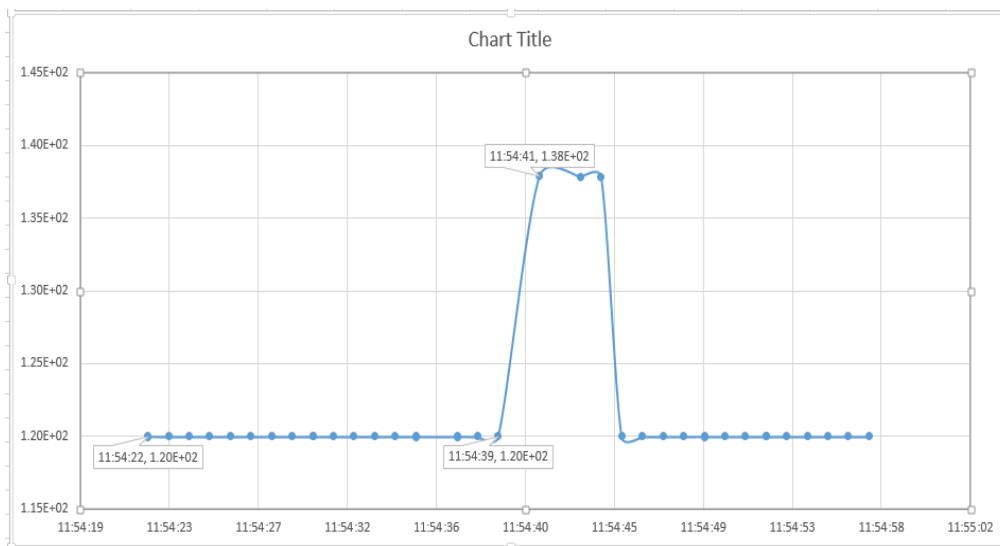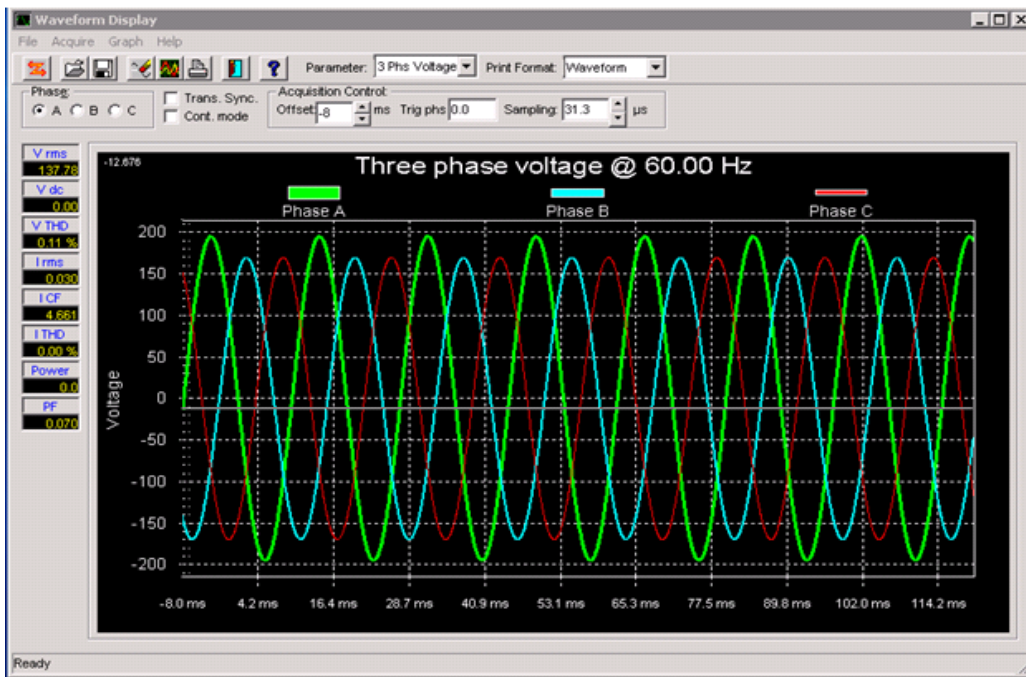for 50% <V<80% Vnominal

Case 3:

Figure 4.18: Voltage fluctuations provided by RS90 and the tripping behavior of the inverter (excel grpah)
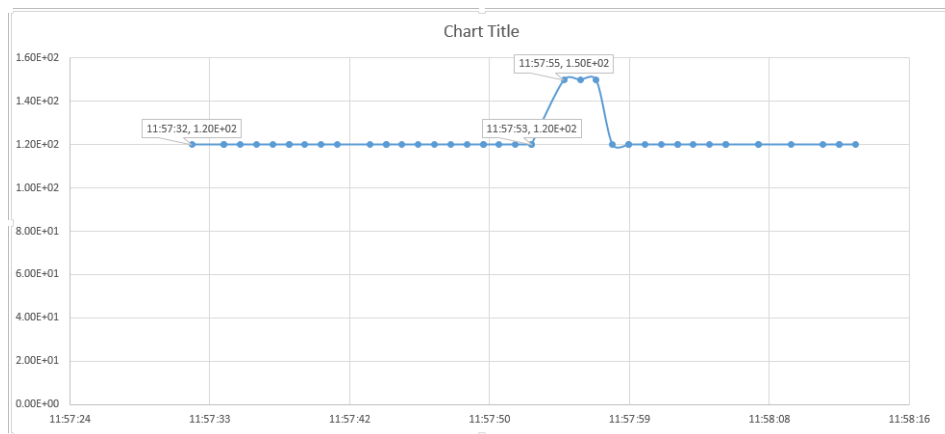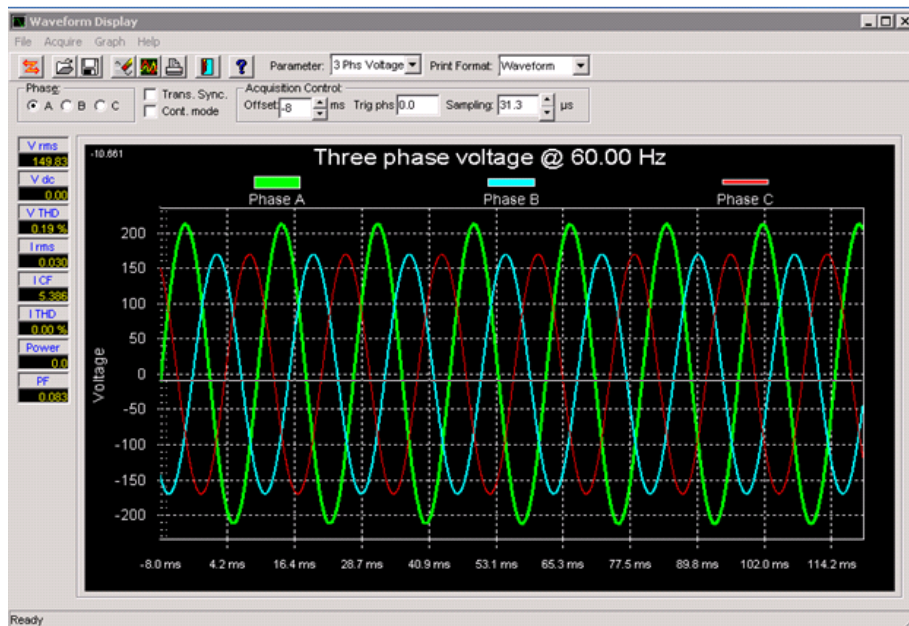
for 80% <V<110% Vnominal

Case 4:

V>120% for 3 seconds

Figure 4.19: Voltage fluctuations provided by RS90 and the tripping behavior of the inverter (excel grpah)

for 120% Vnominal <V

Here we have taken a reference 3 seconds of Voltage step change because it is more than the required maximum clearing time for any mentioned specifications. (Except the excel graph which is just to see the transition)

The voltage anomalies as seen in the figure 4.14, were generated by the power amplifier to test the inverter for disconnection during voltage fluctuation. We noticed that on all the occasions the voltage changes cause the inverter to trip and disconnect from the grid. The inverter waits for the anomaly to pass as seen in the graph, but trips if the voltage maintains itself beyond the allowable range for more than 0.1 sec on all the cases. This is well below the IEEE 1547 guidelines for the trip times for voltage abnormalities.

Frequency variations according to IEEE 1547:

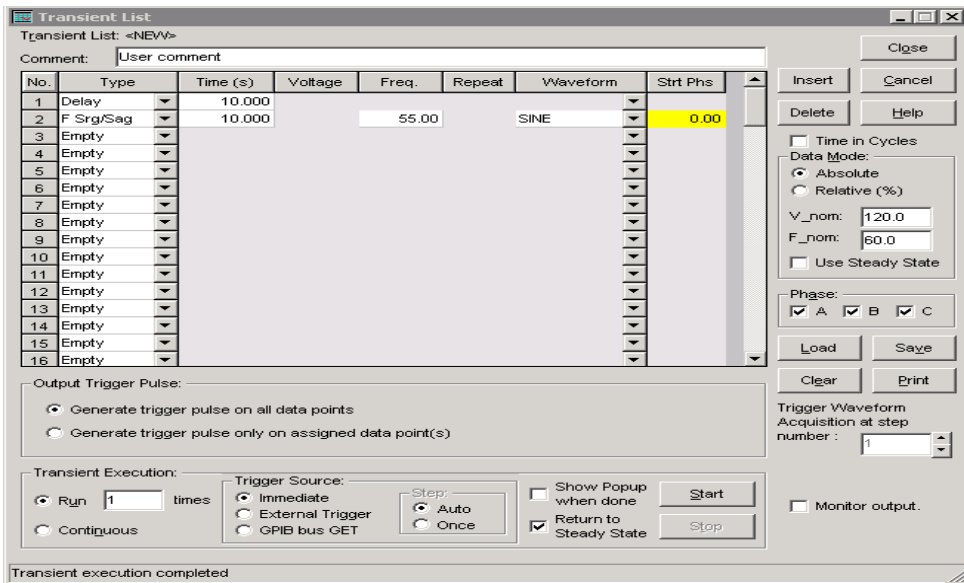Case 1: Let us take an example of F<57 with max clearing time of 0.16 seconds
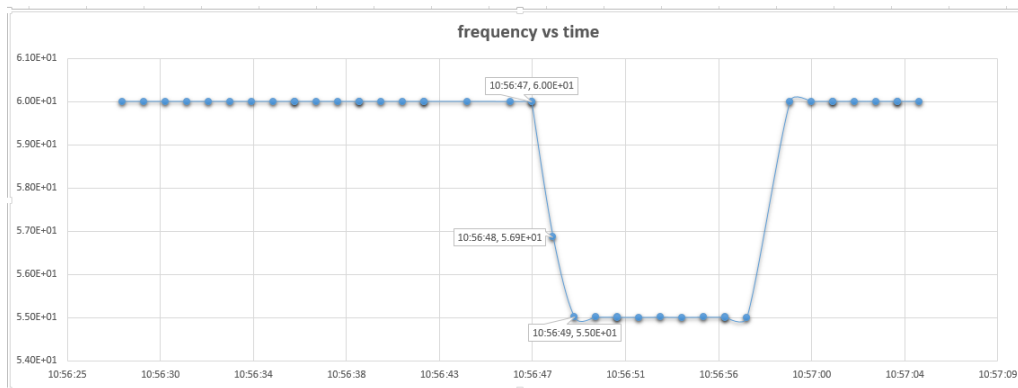

Figure 4.20: The frequency fluctuation program in RS90

Figure 4.21: The tripping behavior of the inverter for F<57 Hz

The inverter tries to remain integrated with the grid for some time before tripping out, but eventually the abnormality duration exceeds the limit and we see the graph shoot up to 60 Hz.
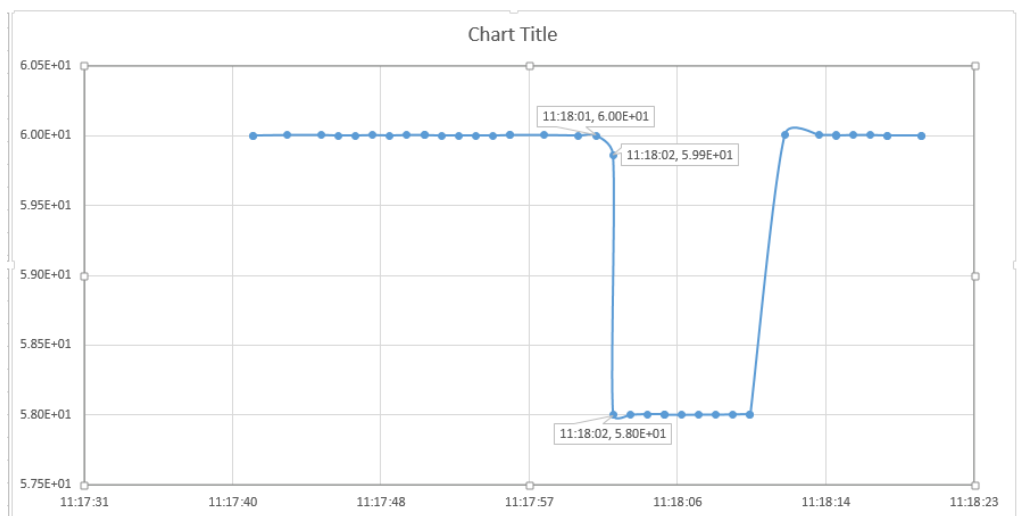
Case 2:

For 57< f <59.8

Figure 4.22: The tripping behavior of the inverter for 57< F<59.8 Hz

Case 3:

For f>60.5

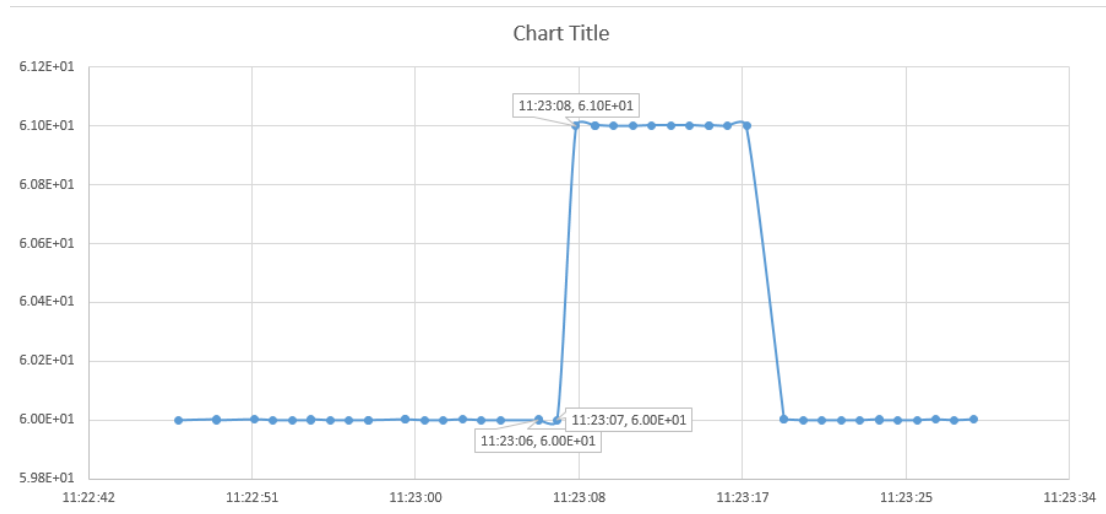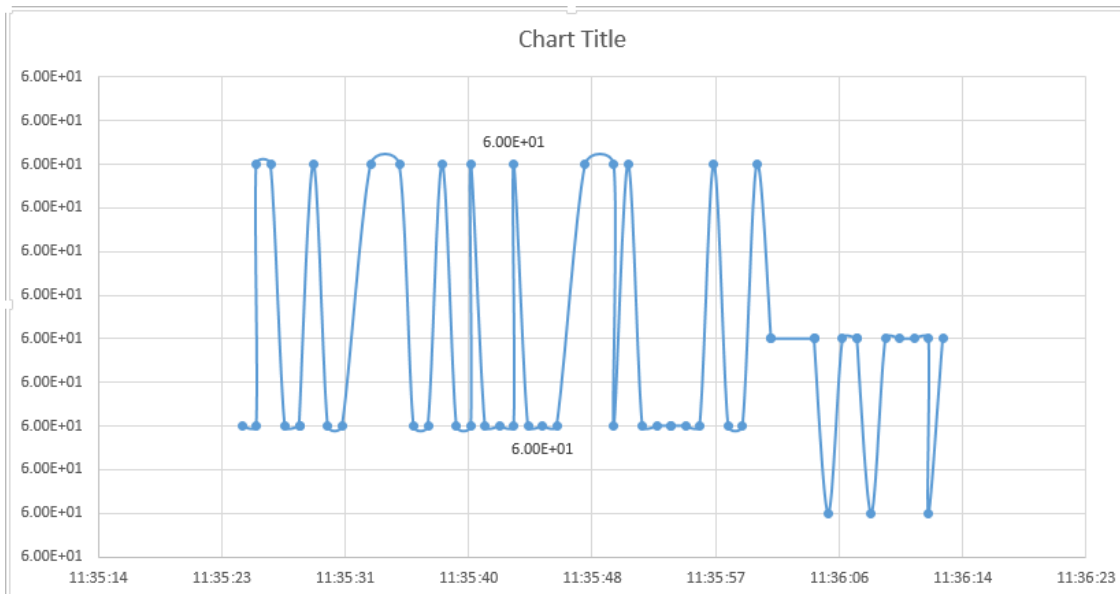

Figure 4.23: The tripping behavior of the inverter for F>57 Hz

Figure 4.13 shows the cases when the frequency of the system is <50 Hz and >60.5 Hz. It is seen that the PV allows this anomaly to exist for a certain period of time before disconnecting from the grid altogether. The disconnection time is <0.2 seconds which is in compliance to the IEEE 1547 standards.

Problems:

1) The transition time is 1-2 seconds here, from nominal to the specified %fnominal. Acquiring the exact values corresponding to precise time stamps will be difficult as the power analyzer has a minimum data acquiring time of 0.2 seconds. If we have a frequency fluctuation which ranges in milliseconds we will not be able to acquire the data at that particular time.

For example, when we have a frequency change from the nominal to 61 Hz for a duration of 0.1 seconds, we have:

Probable solution:

1) Using a different channel we can monitor the inverter side frequency and superimpose the graphs with each other, which might give us a good enough idea about the trip timings.

2) An internal or external timer which can give us any form of information about the event timings can be helpful in this case.

The power-amplifier can be treated as a grid, because of the fact that it can sink in power generated by any connected source. Figure 4.13 shows the cases when the frequency of the system is <50 Hz and >60.5 Hz. It is seen that the PV allows this anomaly to exist for a certain period of time before disconnecting from the grid altogether. The disconnection time is <0.2 seconds which is in compliance to the IEEE 1547

The voltage anomalies as seen in the figure 4.14, were generated by the power amplifier to test the inverter for disconnection during voltage fluctuation. We noticed that on all the occasions the voltage changes cause the inverter to trip and disconnect from the grid. The inverter waits for the anomaly to pass as seen in the graph, but trips if the voltage maintains itself beyond the allowable range for more than 0.1 sec on all the cases. This is well below the IEEE 1547 guidelines for the trip times for voltage abnormalities.

4.6. Summary

This chapter clearly proves that inverters implemented in grid-connected circuits abide by the IEEE and IEC regulations. We were able to dissect the distribution network provided in [6], and mathematically modelled the one house and two house systems which can be further tested on our RTDS platform with real inverters, like the one mentioned in the chapters. The idea is to provide a foundation for future detailed power quality analysis with a real PV inverter system with our VP4 distribution network and hardware in loop testing of IEEE 1547 standards for inverters.

CHAPTER 5 DQ-CONTROL OFF- AND ON-GRID

This chapter involves the results of our off-grid and on-grid application of the dq-control architecture on our inverter system. The simulation was based on a constant irradiation and temperature, and off-grid and on-grid has the load connected at its PCC which was modeled in Chapter 4.

5.1. Overview

The PV inverter system is connected to the load and an off-grid operation takes place. The PLL used here to synchronize it with the grid voltage uses an external power source, we do this in order to generate our orthogonal components. As discussed earlier, the generation of dq-components uses the phase from the grid voltage using the phase locked loop. In the case of off-grid operation, the house load is 300W and the capacitance of the house appliances are modelled to be 3uF. The maximum power output from the PV is 1kW and the voltage base on the system is 230V.

5.2. Power Reference at 1 Per Unit

The simulation parameters are given in table 5.1. The power reference for our dq control architecture is given at 3 per unit, which corresponds to 300W, and the reactive power reference was given to be 0 per unit. These references are responsible for our Id and Iq reference generation.

The power supplied by the PV to the load is shown in figure 5.1.

TABLE 5.1: Simulation parameters

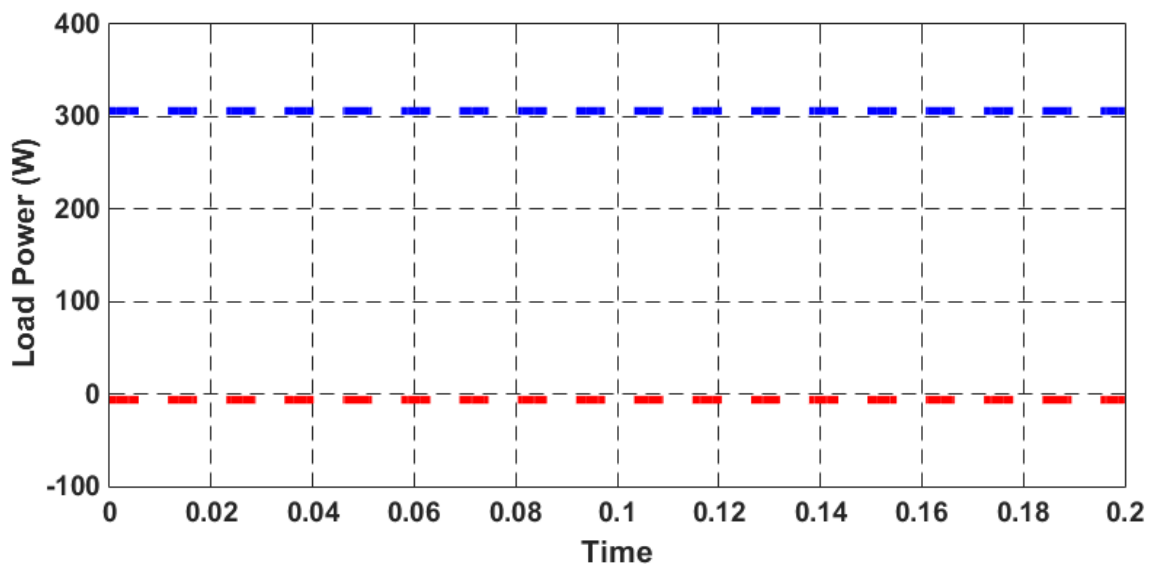| Irradiation	1000 W/m^2
Temperature	25°C
Active power reference	1pu
Reactive power reference	0 pu
Sbase	1 kW
Vbase	230V

FIGURE 5.1: Power supplied by the Photovoltaic

The off-grid application of the implemented dq-control works well for the inverter on the given house load. Figure 5.2 gives us the plot for the voltage and current. RSCAD works on a time step of 50μs, and some disturbances seen on the plot can be ignored. It can be said that a reference of 1 per unit for active power would have resulted similarly because the demanded power is 300W.
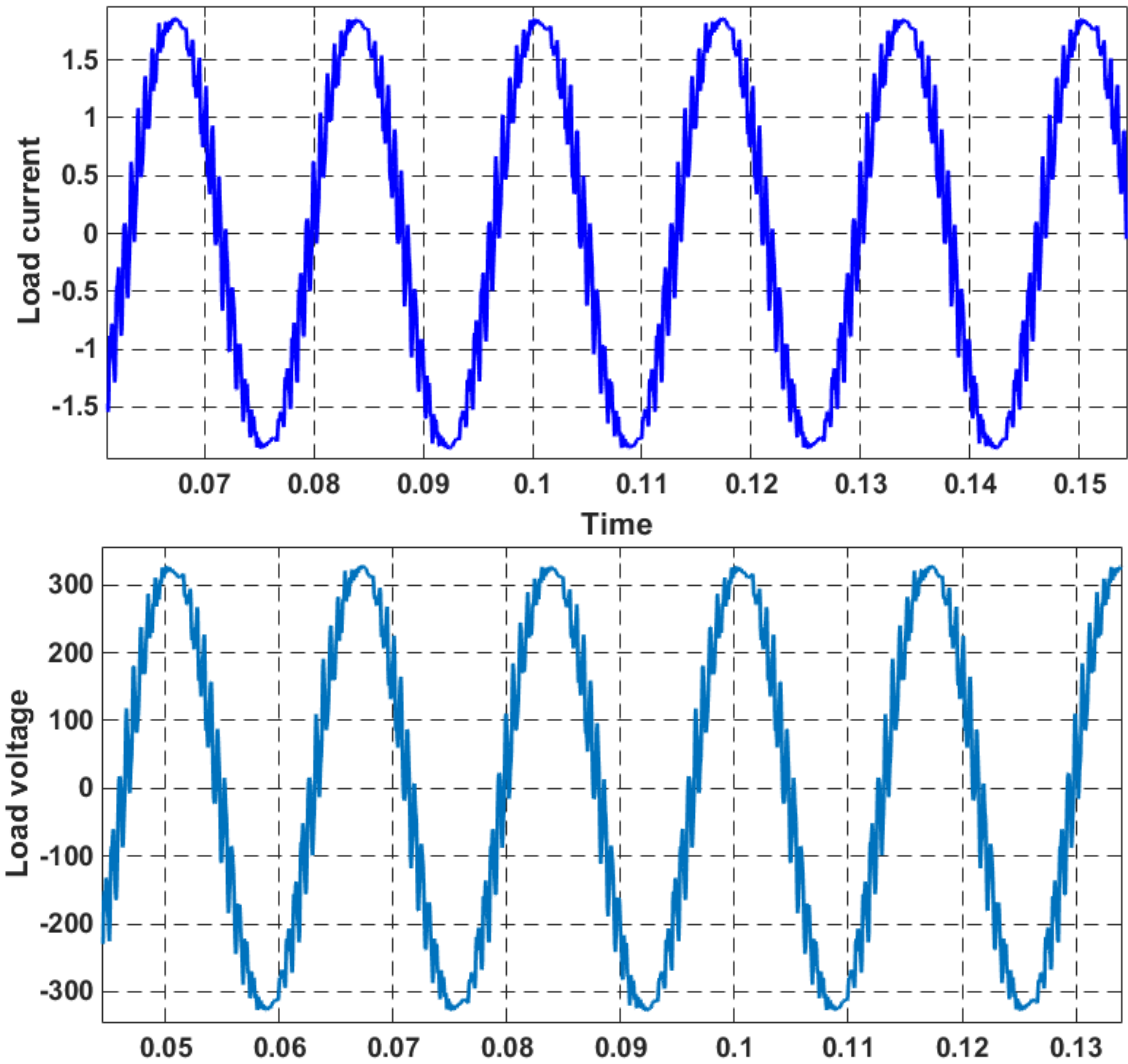
Figure 5.2 Load current and voltage

Controller effort can be seen with the errors reducing or tending to zero in figure 5.3, the values calculated for Kp and Ki in the previous chapters are implemented on the PI controller and the working of this controller can be clearly seen in the figure. We can say that on the off-grid mode of operation the dq-control architecture holds true to its reference set points.
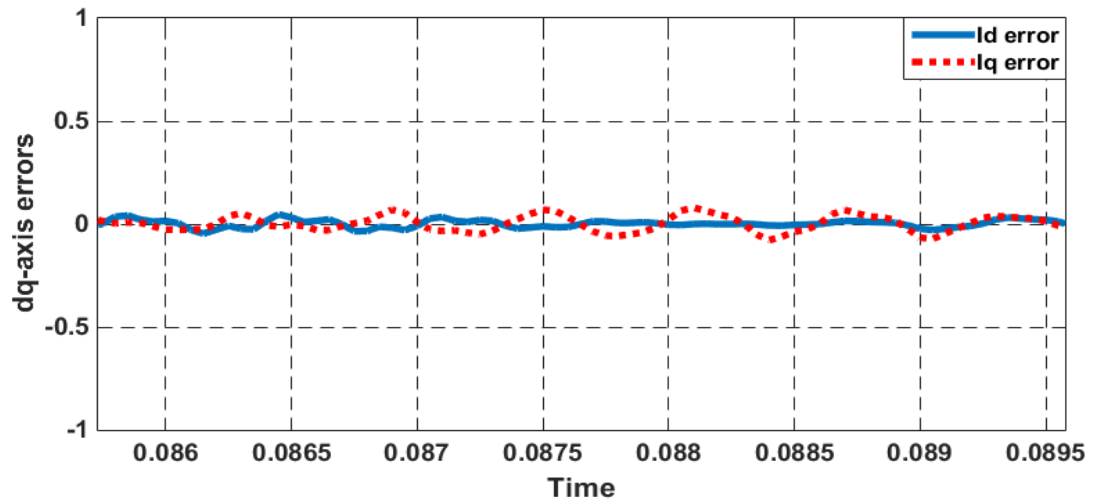
FIGURE 5.3: dq-axis current error signals

5.3. On-Grid Simulation of the DQ-Control Architecture

The PV inverter system are grid-connected in this sub chapter, the gird utilized here is just a simple AC source as of now, because the functionality and robustness of the dq architecture can be recognized by doing this and we can move on to integrate this system to the distribution network.

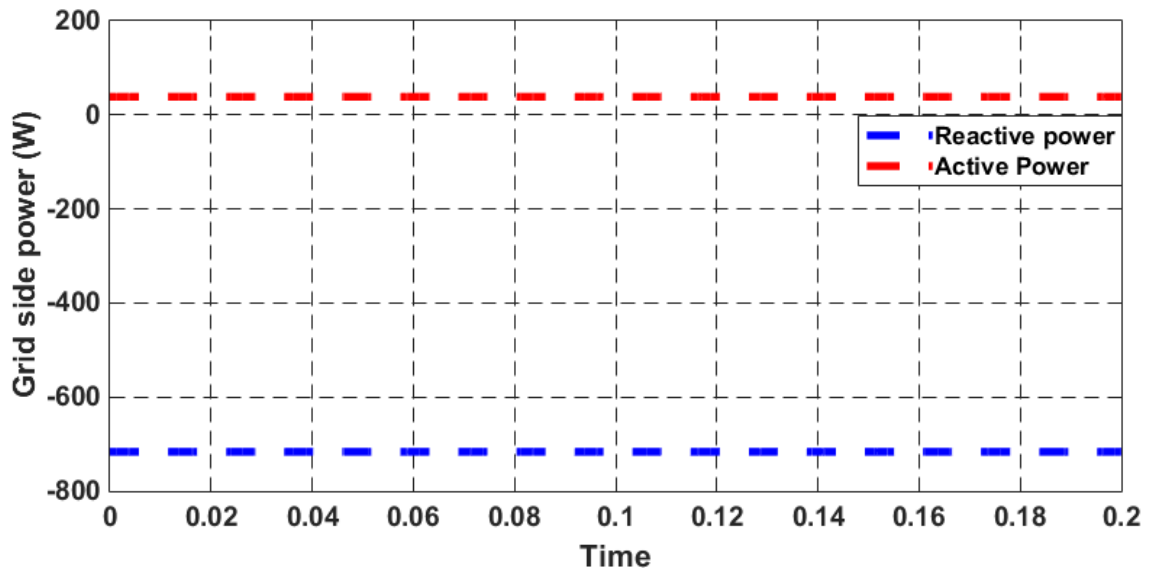FIGURE 5.4: Power on the grid side

Figure 5.4 shows the power transmitted to the grid by the PV inverter system. The power reference for the dq controller architecture is 1 per unit or 1 kW, which the PV abides to as shown in figure 5.5. The load connected at the PCC consumes its demanded power which is shown in figure 5.6
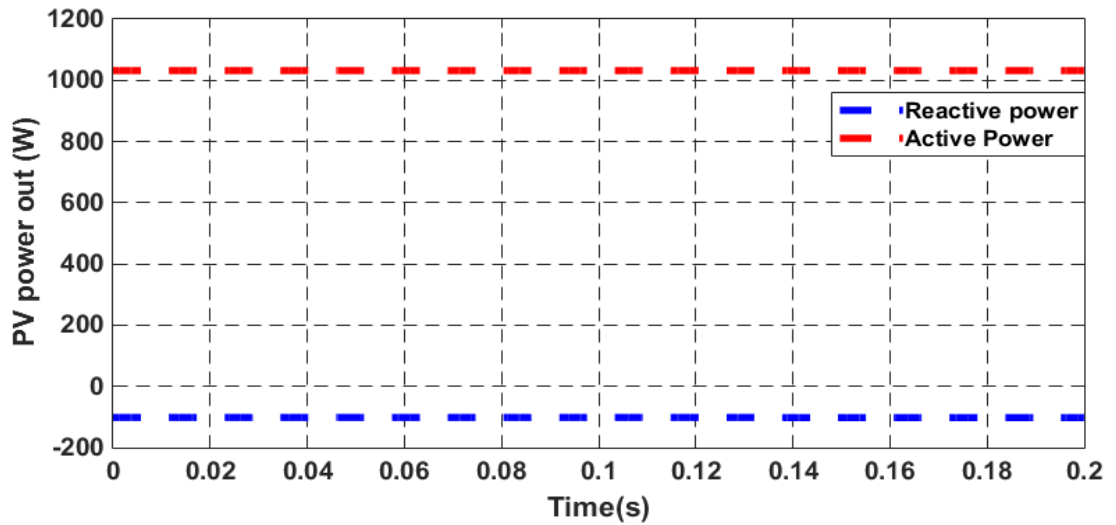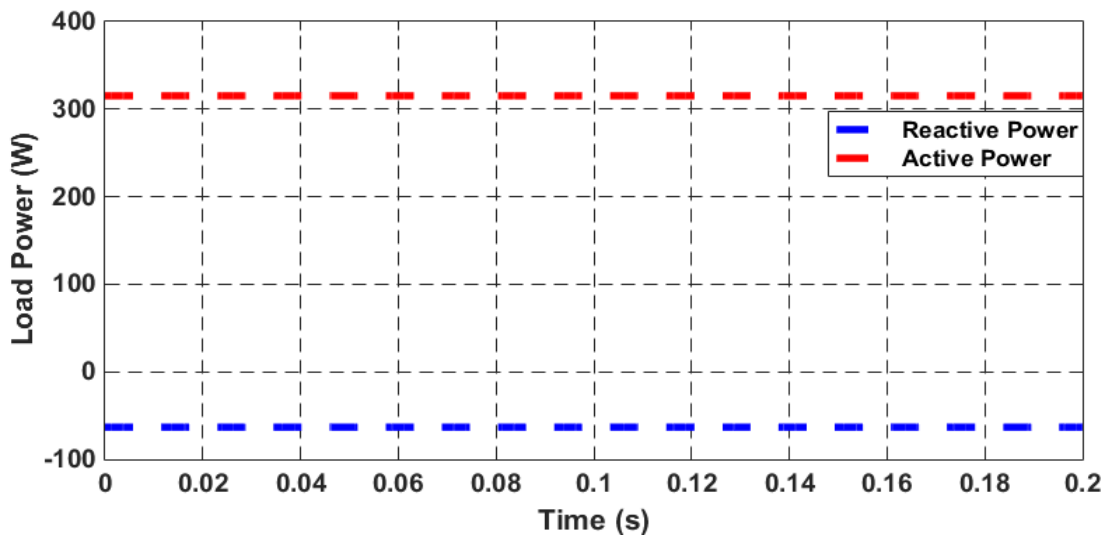

FIGURE 5.5: Power output from the PV

FIGURE 5.6: Power consumed by the load at PCC

5.4. Integration with the Distribution System

5.4.1. Simulation Results

Overview of the distribution network is given in figure 4.8, the interconnection of the PV inverter system was simulated on RSCAD and the results are provided in the figures 5.7 and 5.8. The off-grid mode was first allowed to be operated for the voltage at the output of the inverter to be 230V, and synchronized with the grid. During the operation the load powers and the output powers are shown. When the grid is connected to the system, the PV starts supplying to the grid as shown in the figure 5.8. Although we see some minor changes on the secondary side voltage, the power supplied by the PV is 1kW.
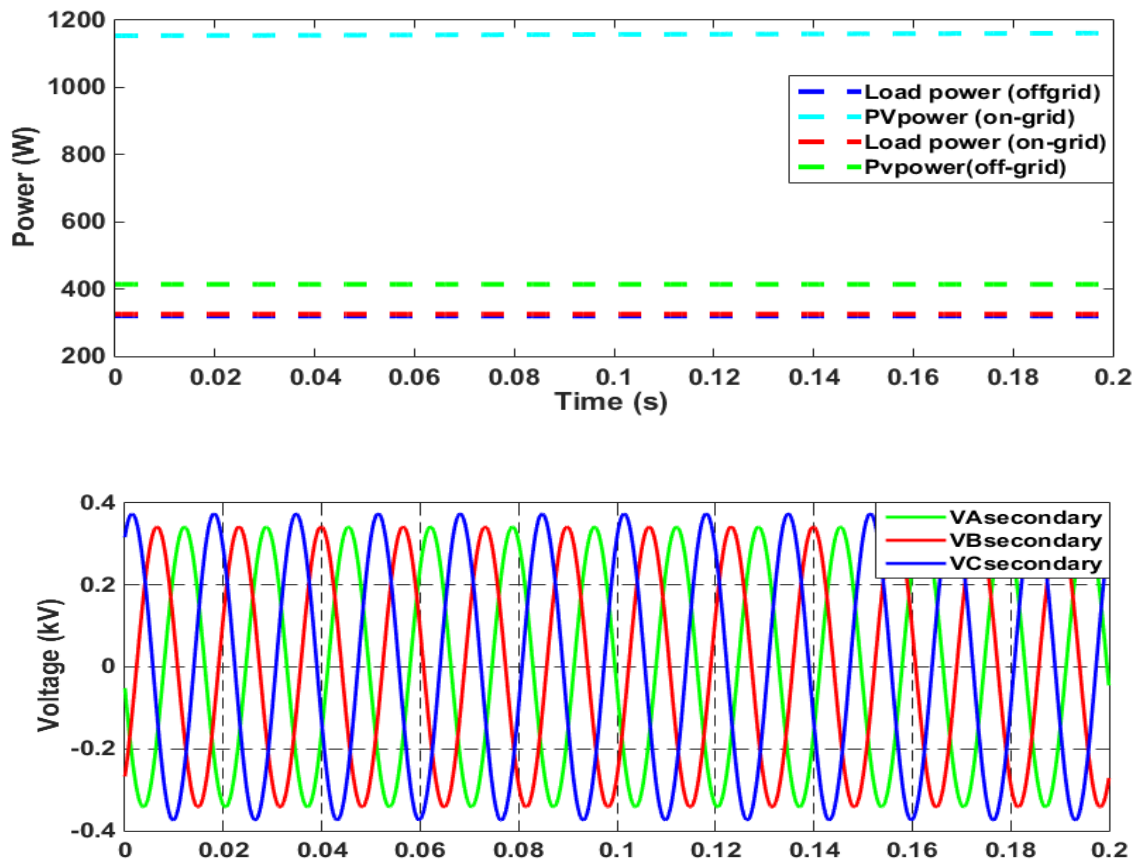

FIGURE 5.7: Voltage waveforms for on-grid operation on the secondary side and power transfer during on and off grid operations
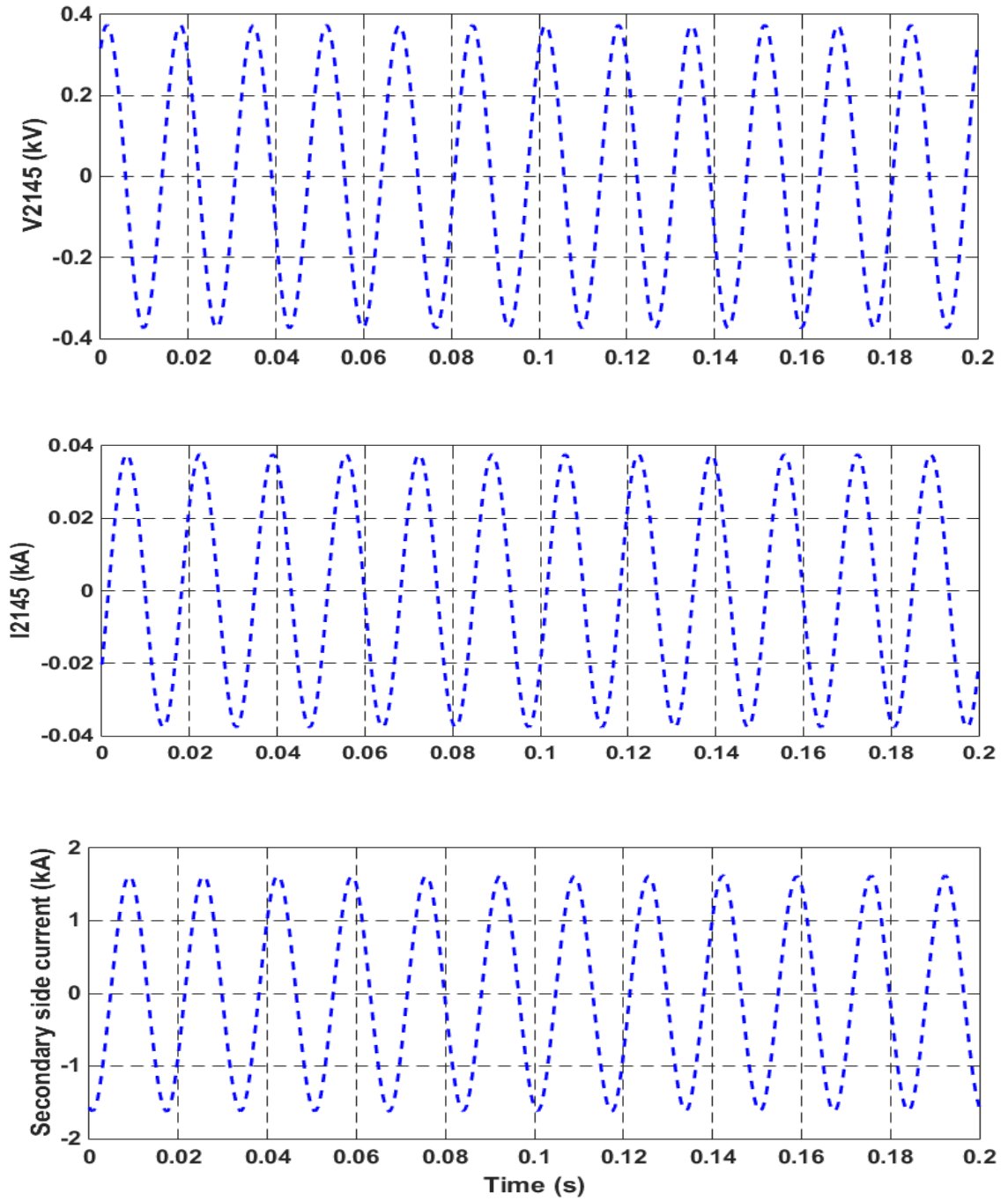
FIGURE 5.8: voltage at the secondary side, on-grid operation current of 2145 branch and current on the

secondary side of the transformer

5.4.2. Harmonic Analysis

The harmonic analysis in RSCAD is done by a frequency sweep on the primary side of the transformer. Figure 5.9 shows the impedance during the sweep and we can evaluate that the system resonance occurs at around 2000Hz, this is around the 33rd harmonic.
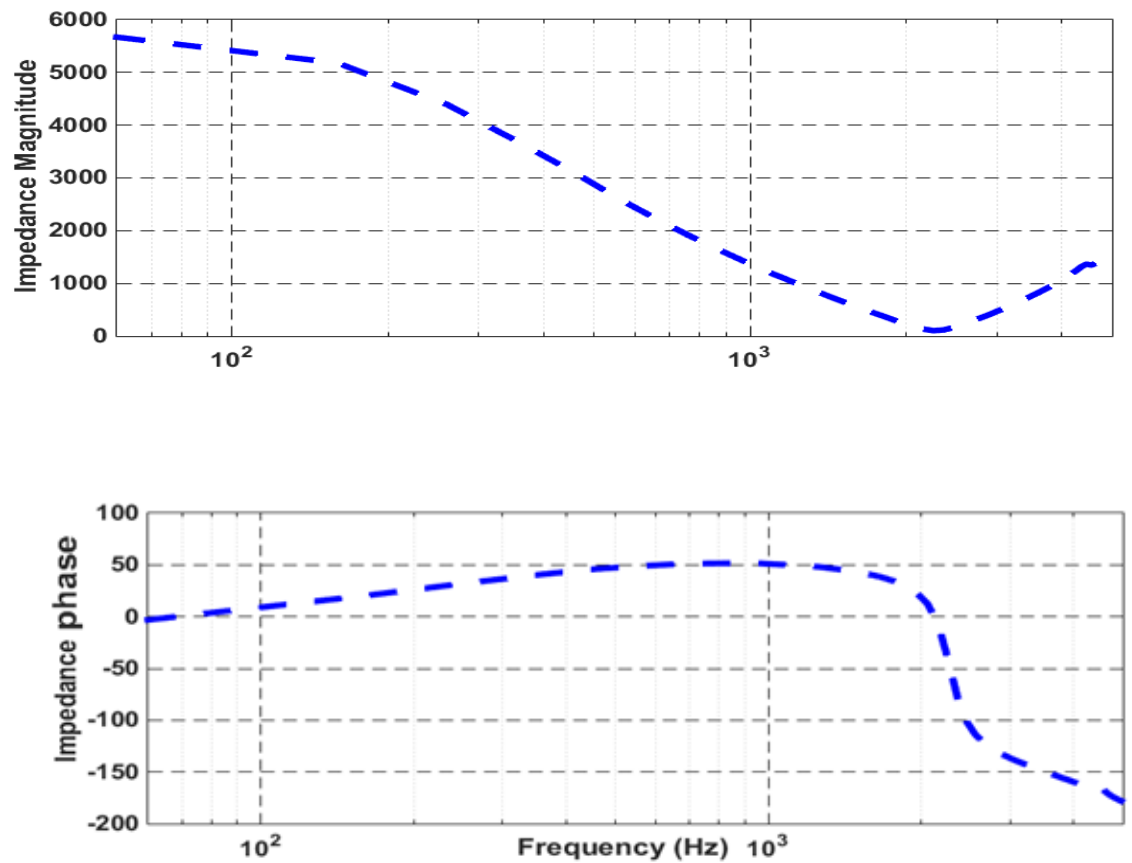
FIGURE 5.9: Impedance on the secondary side of the transformer during frequency sweep

The VP4 network modelled in RSCAD was then evaluated on different THD levels using the same process by doing a frequency sweep on the secondary side voltage, current and Bhe house voltage and current. Figure 5.10 shows the harmonic content on the secondary side of the transformer in figure 4.1 and on the 2145Bhe house with 2% THD.

We notice that the higher harmonics, close to the 30th harmonic are the dominant ones. Although we see some of the lower level harmonics (on the PCC and the secondary side) to be quite dominant, we can safely say that the higher voltage harmonics are more dominant and they can be seen to be peaking.
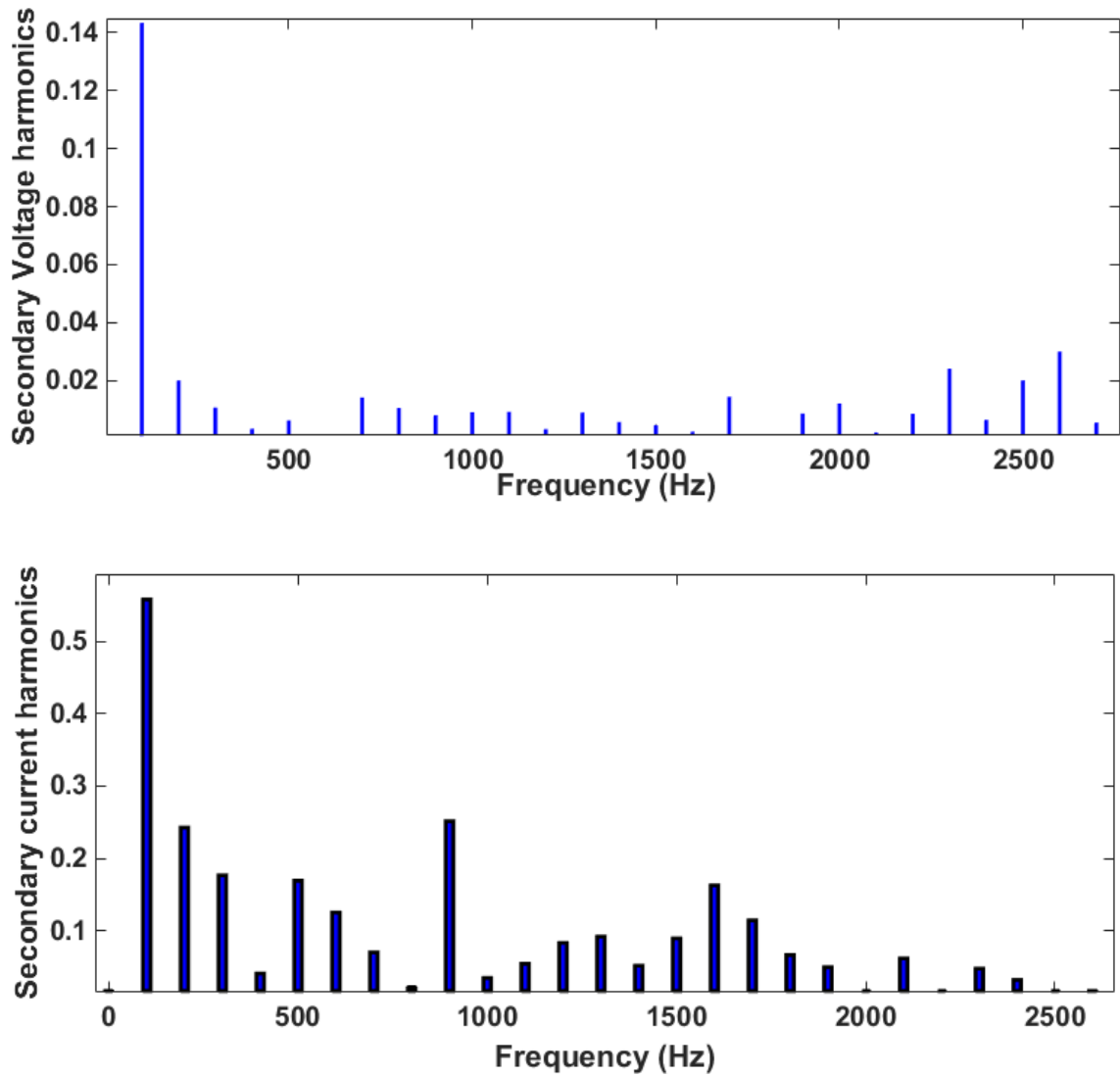
FIGURE 5.10: Voltage and current harmonics for average THD of 2% on the secondary side of the transformer (on the side of the distribution network)
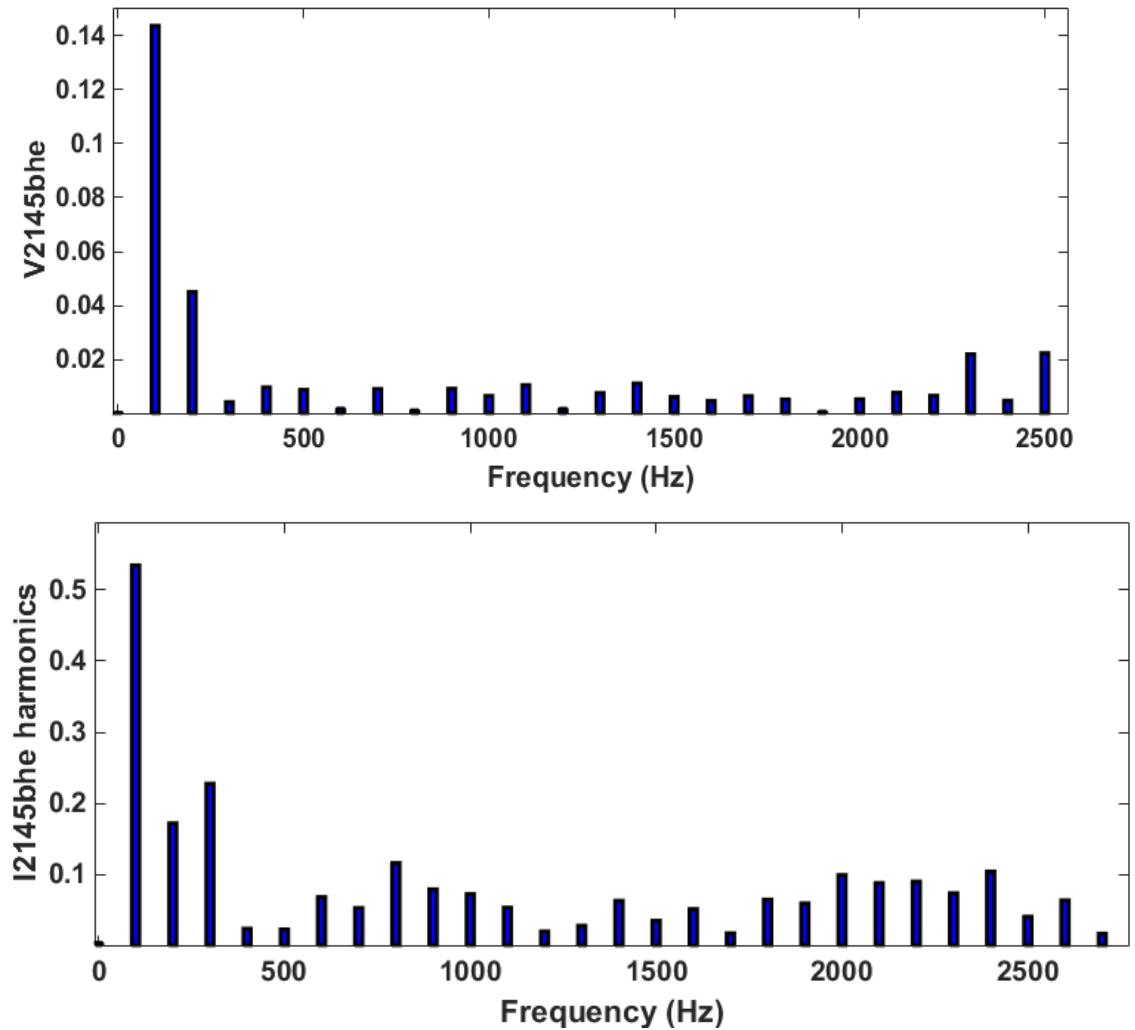
FIGURE 5.11: Voltage and current harmonic for average THD of 2% at 2145Bhe house

The same thing was observed as the THD worsened. At >8% THD, which is not allowable generally, we see that the dominant voltage harmonics are seen to occur at 3000Hz on the secondary side and the PCC of 2145Bhe. This particular range of harmonics is not same as [6], but it is very close to the calculated value which excludes the presence of 18 rooftop PVs in [6]. We can further say that as and when the PV penetration is increase, there is a possibility of these harmonics at the resonant frequency to peak and cause severe damage to the system.
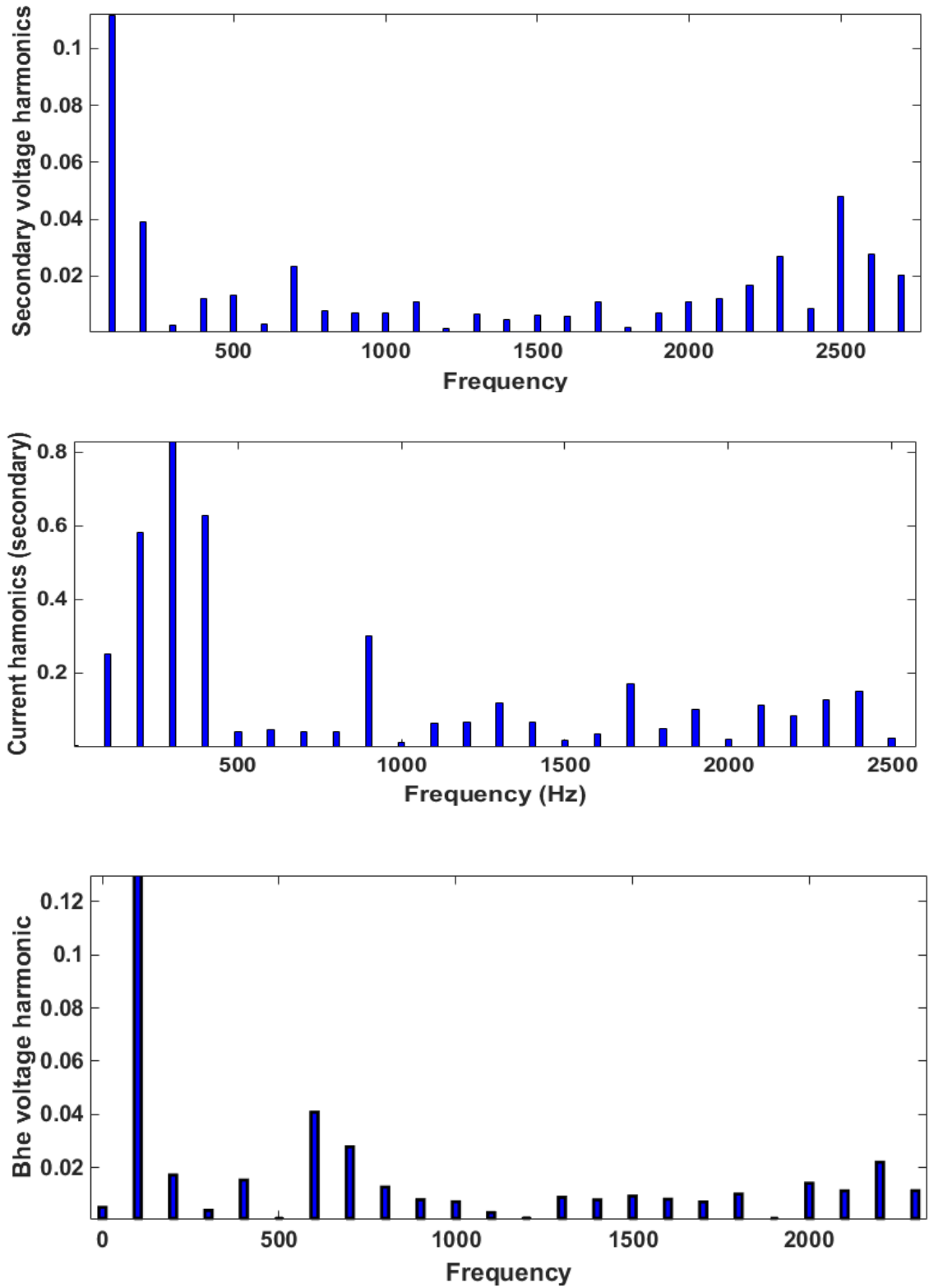
FIGURE 5.11: Voltage and current harmonic for 8% THD at a) the secondary side of the transformer b)

2145Bhe house

5.5. Summary

This chapter not only focuses on providing the results for the dominating harmonics and the validation for DQ-control strategy on the inverter, but also gives us an idea about the severity in the ignorance of the higher level harmonics in distribution system. If these harmonics are not eliminated, the increasing PV penetration might lead to a catastrophic event when these higher level harmonics are fed to their maximum. Right now, the dominance is observable, but feeding in more might cause abrupt tripping of inverters in distribution networks, because the feeder transformers usually are modelled in a way that do not allow harmonics to travel to the other side. Due to this, these harmonics might stay in the network and become exaggerated. This model, serves the purpose of future studies as well, on power quality and harmonic elimination methodologies.

CHAPTER 6 : CONCLUSION AND FUTURE WORKS

6.1. Conclusion

- VP4 network was built in RSCAD and validated by the results provided in [6] and one house rooftop PV system was created in RSCAD. PV inverter system was tested for IEEE standards on grid interconnection.

- DQ-control methodology was investigated and implement on the single phase H-bridge inverter on the one house rooftop PV system in the VP4 network built in RSCAD. The 90-degree phase shift method proved to be useful in generating the dq-components of the inverter system. The Simulation results from RSCAD closely match our mathematical calculation derived from [6] of the one house rooftop PV-distribution system.

- Dominant harmonic generation was studied and compared to [6]. It was seen that the results are closely linked and a slight change in the dominating harmonics is considered to be due to the fact that there is only one PV on the system compared to 18 rooftop PVs on the VP4 network referred in [6].

- Simulation results provided an insight on the capability of inverter towards generation and contribution towards harmonics. The distribution network saw the peaking of certain harmonics; this amplification is due to the presence of the resonating network.

- Not only this, ignoring these harmonics might be catastrophic if the PV penetration is increased which might be equivalent to providing a vessel for these harmonics to exist in and even exaggerate itself.

6.2. Future Works

- The system can be further built up to 3 houses and tested on a hardware platform using the hardware in loop (HIL) property of RSCAD and a detailed investigation can be performed on irradiance changes and other system dynamics.

- Active power filtering methodologies can be implemented and different estimation techniques can be implemented to compare the efficiency and range of filtering for different technique.

- Other control strategies can be investigated by implementing on this platform and their behavior can be compared in regards to generation of harmonics, output voltage control, active-reactive power control etc.

BIBLIOGRAPHY

[1] G.J. Naaijer, 'Transformer-less inverter cuts photovoltaic system losses," *Electronics,* pp.121-122, Aug. 1980

[2] J. Arrillaga, D.A. Bradley, and P.S. Bodger, *Power System Harmonics.* New York: Wiley, 1985.

[3] J. Myrzik, "Power conditioning of low-voltage generators with transformerless gridconnected inverter topologies," in *Proc. 7th Eur. Conf. Power Electronics Applications (EPE'97)*, Trondheim Norway, 1997.

[4] M. Calais, J. Myzrik, T. Spooner, and V.G. Agelidis, "Inverters for single-phase grid connected photovoltaic systems-An overview' in *Proc. 33th IEEE Power Electronics Specialists Conf. (PESC'02),* Cairns, Australia, June 23-27, 2002.

[5] A. Kostsopoulous, P.J.M Heskes, and M.J. Jansen, "Zero-crossing distortion in grid-connected PV inverters," in *Proc. 28th IEEE Industrial Electronics Conf. (IECON'02),* vol.1, Sevilla, Spain, Nov. 5-8,2002, pp.1-6

[6] J.H.R. Enslinm W.T.J. Hulhorst, A.M.S. Atmadji, P.J.M. Heskes, A. Kostsopoulos, J.F.G. Cobben, and P. Van der Sluijs, "Harmonic interaction between large numbers of photovoltaic inverters and the distribution network," in *Proc. IEEE Power Technol. Conf.,* Bologna, Italy, June 23-26, 2003.

[7] P.J.M. Heskes and J.H.R Enslin, "Power quality behavior of different photovoltaic inverter topologies," in *Proc. 24th PCIM Conf. (PCIM'03),* Numeberg, Germany, May 20-22, 2003.

[8] S.A.M. Verhoeven, "Impacts of PV penetration in distribution networks," in *Proc. IEA task V Workshop,* Jan. 24-25, 2002.

[9] C.Wang and M.H.Nehrir, "Power management of a stand-alone wind/ photovoltaic/fuel cell energy system," *IEEE Trans. Energy Convers.*, vol. 23, no. 3, pp. 957–967, Sep. 2008.

[10] S. Buso, L. Malesani, P. Mattavelli, "Comparison of Current Control Techniques for Active Filter Applications", IEEE Transaction on Power Electronics, Vol. 13, Jan. 1998, pp. 179-185

[11] S.B. Kjaer, J.K. Pedersen, and F. Blaabjerg, "A review of single-phase grid-connected inverters for photovoltaic modules," IEEE *Trans. Ind. Appl.,* vol. 41, no. 5, pp. 1292-1306, Sep./Oct. 2005.

[12]   S.-G. Jeung and M.H. Park," The analysis and compensation of dead-time effects in PWM inverters," *IEEE Trans. Ind. Electron.,* vol. 38, no.2, pp.108-114, Apr. 1991

[13]   *IEEE Recommended Practices and Requirements for Harmonic Control in Electrical Power Systems, IEEE Standard 519-1992,1992.*

[14]   *IEEE Standard for Interconnecting Distributed Resources with the Electric Power System,* IEEE Standard 1547-2003, 2003.

[15]   J.A. Orr and A.E. Emanuel, "On the need for strict second harmonic limits," IEEE Trans. Power Del., vol. 15, no.3, pp. 967-971, Jul. 2000.

[16]   Moran, L.; Fernandez, L.; Dixon, J.; Wallace, R, "A simple and low cost control strategy for active power filters connected in cascade", IEEE Transactions on Industrial Electronics, Vol. 44, No. 5, October 1997

[17]   F. Franchetti, H. Karner, S. Kral, and C. W. Ueberhuber, "Architecture independent short vector FFTs," in Proc. IEEE Int'l Conf. Acoustics, Speech, and Signal Processing, vol. 2, 2001, pp. 1109–1112.

[18]   Moran, L.; Fernandez, L.; Dixon, J.; Wallace, R, "A simple and low cost control strategy for active power filters connected in cascade", IEEE Transactions on Industrial Electronics, Vol. 44, No. 5, October 1997

[19]   Moran, L.; Fernandez, L.; Dixon, J.; Wallace, R, "A simple and low cost control strategy for active power filters connected in cascade", IEEE Transactions on Industrial Electronics, Vol. 44, No. 5, October 1997

[20]   Moran, L.; Fernandez, L.; Dixon, J.; Wallace, R, "A simple and low cost control strategy for active power filters connected in cascade", IEEE Transactions on Industrial Electronics, Vol. 44, No. 5, October 1997

[21]   Moran, L.; Fernandez, L.; Dixon, J.; Wallace, R, "A simple and low cost control strategy for active power filters connected in cascade", IEEE Transactions on Industrial Electronics, Vol. 44, No. 5, October 1997

[22]   N. Maruin, A. Alam and S. Mahmod, and H. Hizam, "Review of control strategies for power quality conditioners," in proc. of IEEE PECon 2004, pp.109-115, Nov. 200

[23]   L. Asiminoaei, F. Blaabjerg, and S. Hansen, "Detection is key— Harmonic detection methods for active power filter applications," IEEE Ind. Appl. Mag., vol. 13, no. 4, pp. 22–33, Jul.Aug. 2007.

[24]   M.El-Habrouk, M. K Darwish and P. Mehta, "Active power filters: a review,"
        IEE Proc- Electric Power Applicrrtions. vol: 147, Issue: 5, pp. 403-413, Sept.
        2000.

[25]   J. H. R Enslin, J. D. Van Wyk, "A new control philosophy for power electronic
        converters as fictitious power compensators," IEEE Transaction on Power
        Electronics. Vol. 5, issue. 1, pp 88-97, Jan. I990

[26]   J. T. B. A. Kessels, M. Koot, B. de Jager, P. P. J. Van Den Bosch, N. P. I. Aneke,
        and D. B. Kok, "Energy management for the electric powernet in vehicles with a
        conventional drivetrain," IEEE Trans. Control Syst. Technol., vol. 15, no. 3, pp.
        494–505, May 2007

[27]   S. Luo, Z. Hou "An adaptive detecting method for harmonic and reactive
        currents" IEEE Trans. on Industrial Electronics, Vol. 42, Issue. 1, pp. 85 –89,
        Feb. 1995.

[28]   M. T. Haque, S. H. Hosseini and T. Ise, "A control strategy for parallel active
        filters using extended p-q theory and quasi instantaneous positive sequence
        extraction method," in proc. ISIE 2001. Puson, Korea. pp. 348-353

[30]   A. Nabae, H. Nakano and S. Togasawa, "An instantaneous distortion current
        compensator without any coordinate transformation," in Proc. IEEJ Int. Power
        Electro. Conf. (IPEC-Yokohama), 1995, pp. 1651 1655.

[31]   M. K.Mishra, A. Ghosh, and A. Joshi, "Operation of a DSTATCOM in voltage
        control mode," IEEE Tran. Pow.Del., vol. 18, pp.258-264, Jan.200

[32]   A. Abellan. G. Garccra, M. Pascual, E. Figucrcs, "A new current controller
        applied to Four-brach inverter shunt activc filters with UPF control method,"
        IEEE 32nd AnnuaI Power Elccrronics Specialist Conference, 2001, vol. 3. pp.
        1402-1407

[33]   A. Abellan. G. Garccra, M. Pascual, E. Figucrcs, "A new current controller
        applied to Four-brach inverter shunt activc filters with UPF control method,"
        IEEE 32nd AnnuaI Power Elccrronics Specialist Conference, 2001, vol. 3. pp.
        1402-1407

[34]   A. Banerji, S. K. Biswas and B. Singh, "DSTATCOM control algorithms: A
        review," International Journal of Power Electronics and Drive System (IJPEDS)
        Vol.2, No.3, pp. 285-296, September 2012.

[35]   A. Chandra, B. Singh, B. N. Singh and K. Al-Haddad, "An improved control
        algorithm of shunt active filter for voltage regulation, harmonic elimination,
        power-factor correction, and balancing of nonlinear loads", IEEE Transactions On
        Power Electronics, vol. 15, No. 3, pp. 495-507, May 2000.

[36] B.S. Rajpurohit and S.N. Singh "Performance Evaluation of Current Control Algorithms Used for Active Power Filters", in proc of EUROCON 2007, The International Conference on "Computer as a Tool", pp. 2570-2575, 2007

[37] A. Ghosh, A. K. Jindal and A. Joshi, "Inverter Control Using Output Feedback for Power Compensating Devices," in Proc. TENCON 2003, vol. 1, pp.48-52, Oct.2003

[38] Y.Xue, L. Chang, S.B. Kjær, J. Bordonau, and Toshihisa Shimizu, "Topologies of Single-Phase Inverters for Small Distributed Power Generators: An Overview ," IEEE Transactions on Power Electronics, vol. 19, pp. 1305-1314,.Sept. 2004

[39] F. Blaabjerg, R. Teodorescu, M. Liserre, and A. Timbus, "Overview of control and grid synchronization for distributed power generation systems," Industrial Electronics, IEEE Transactions on, vol. 53, no 5, pp. 1398-1409, Oct. 2006.

[40] M.J. Ryan and R.D. Lorenz, "A synchronous-frame controller for a single phase sine wave inverter," in Proceedings of Applied Power, Electronics Conference., Vol. 2, pp. 813-819, 1997.

[41] R. Zhang, M. Cardinal, P. Szczesny, and M. Dame, "A grid Simulator with Control of Single-Phase Power Converters in D-Q Rotating Frame," Power Electronics Specialists Conference, Vol. 3, pp. 14311436, 2002.

[42] M. Gonzales, V. Cardenas and F. Pazos, "DQ Transformation Development for Single-Phase Systems to Compensate Harmonic Distortion and Reactive Power," 9th IEEE International Power Electronics Congress, pp. 177-182, 2004.

[43] S. Silva, B. Loopes, B. Filho, R. Campana, and W. Bosventura, "Performance evaluation of pll algorithm for single-phase grid connected systems," Industry Applications Conference, 2004, 39th IAS Annual Meeting, Conference Record of the 2004 IEEE, vol. 4, pp. 2259-2263, Oct. 2004

[44]   H.R. Karshenas, H. Saghafi, "Basic Criteria in Designing LCL Filters for Grid Connected Converters," IEEE International Symposium on Industrial Electronics, Vol. 3, pp. 1996-2000, 200

[45] U.A. Miranda and L.G.B. Rolin, "A DQ Synchronous Reference Frame Current Control for Single-Phase Converters," Power Electronics Specialists Conference, pp. 1377-1381, 2005.

[46] Jasim Farhood Sultani, "Modelling, Design and Implementation of D-Q Control in Single Phase Grid-connected Inverters for Photovoltaic Systems Used in Domestic Dwellings.", Doctor of Philosophy Thesis, De Monfort University, Leicester, UK.

[47] M. Singh, V. Khadkikar, A. Chandra, R.K. Varma, "Grid Interconnection of Renewable Energy Sources at the Distribution Level With Power-Quality Improvement Features," IEEE Transactions on Power Delivery, vol.26, no.1, pp.307-315, Jan. 2011.